*Journal of Industrial and Management Optimization*

JIMO, 22(12): 6166–6212.
DOI: 10.3934/jimo.2026208
Received: 22 September 2026
Revised: 23 October 2026
Accepted: 29 October 2026
Published: 05 November 2026

https://www.aimspress.com/journal/jimo

*Research article*

# Conditional effects of network position, payoff uncertainty, and strategic inertia on supply chain greenwashing evolution

**Xianrong Hu[1], Haiping Ren[1] and Fan Zhang[2,*]**

[1] School of Business, Jiangxi University of Science and Technology, Nanchang 330013, China
[2] Department of Basic Subjects, Jiangxi University of Science and Technology, Nanchang 330013, China

* **Correspondence:** Email: 9520090006@jxust.edu.cn; Tel: +86-135-7601-4900.

**Abstract:** Greenwashing in supply chain networks is shaped by heterogeneous enterprise relationships, uncertain payoffs, and decentralized strategic interactions. This study develops a network-based evolutionary game model integrating a Barabási–Albert scale-free network, triangular fuzzy payoff representations, degree-dependent strategic inertia, and an inertia-modified Fermi imitation mechanism. A homogeneous mean-field approximation is derived as an analytical benchmark, while repeated Monte Carlo simulations examine the initial strategy's placement, payoff uncertainty, stochastic sampling mechanisms, social learning, network connectivity, and payoff evaluation methods. The baseline mean-field model yields an attracting interior equilibrium at a greenwashing density of 0.8889 under the weighted defuzzified payoffs, which does not directly predict the finite network's outcomes. Numerical results indicate that the initial strategy's placement substantially affects greenwashing diffusion: Assigning 30 initial greenwashing strategies to high-degree, randomly selected, and low-degree enterprises produces mean terminal densities of 0.9609, 0.7744, and 0.3609, respectively. Extreme payoff boundary adjustments significantly increase terminal greenwashing density relative to the baseline, whereas mean-controlled interval width variations do not produce statistically detectable differences. The intensity of social learning and strategic inertia exhibit significant overall effects, but their interaction is not statistically significant under the tested configurations. Furthermore, degree-normalized payoff evaluation attenuates the differences associated with network connectivity, while mechanism ablation experiments indicate that the initial placement's effects depend on payoff evaluation and behavioral assumptions. Overall, the findings highlight the conditional roles of network position, payoff uncertainty, and strategic inertia in the evolution of supply chain greenwashing, providing insights for network-sensitive governance.

**Keywords:** supply chain greenwashing; evolutionary game; fuzzy payoff representations; BA scale-free network; strategic inertia; stochastic payoff sampling
**Mathematics Subject Classification:** 91A86, 90B06, 91A22

## 1. Introduction

Under the global consensus on climate governance and sustainable development, green and low-carbon transformation is profoundly reshaping the underlying logic of economic development. However, real-world supply chain systems are inherently characterized by market uncertainty and network heterogeneity, where firms' decision-making is subject to fluctuating payoffs and topological disparities. In this context, supply chain greenwashing has emerged as a hidden and contagious challenge that undermines the credibility of corporate environmental commitments and complicates genuine green transformation [1]. Its association with interfirm relationships also highlights the need to examine greenwashing beyond isolated enterprises [2,3].

From a micro perspective, the drivers of greenwashing are complex. Financial incentives, information asymmetry, and managerial considerations can influence enterprises' choices between genuine green transformation and opportunistic greenwashing [4,5]. Peer effects and corporate networks may reinforce greenwashing behavior [6,7], whereas digital governance and environmental regulation provide potential constraints [8–10]. Evolutionary game studies have further examined greenwashing incentives and governance under dynamic regulation, financial mechanisms, and information services [11–13]. Nevertheless, many existing greenwashing models focus on interactions among a limited number of representative stakeholders, while the conditional influence of heterogeneous enterprise connections and initial strategy placement remains less explicitly characterized.

Complex network theory provides a powerful tool for characterizing these interactions. Barabási and Albert [14] established the preferential attachment mechanism underlying scale-free networks, while Santos and Pacheco [15] demonstrated the importance of network heterogeneity for cooperative behavior. Nowak and May [16] and Szabó and Fath [17] provided important foundations for evolutionary games on networks. Recent studies have extended network evolutionary analysis to supply chain applications. Zhou and Li [18] examined the co-evolution of information sharing and motivation in complex supply chain networks. Wu et al. [19] investigated green packaging diffusion in logistics enterprise clusters. Chen et al. [20] analyzed green innovation diffusion, while Yang et al. [21] examined blockchain-enabled green supply chain development from a complex-network evolutionary perspective. However, further investigation is needed into how the initial placement of greenwashing across differently connected firms, degree-dependent strategic inertia, local social imitation, and the accumulation of payoff jointly shape evolutionary outcomes. In particular, the effects of network position may depend on the initial strategy configurations and the mechanisms through which firms evaluate payoffs and update their strategies.

In real-world decision-making environments, enterprises' perceptions of key parameters are often vague and imprecise. Fuzzy set theory provides an effective mathematical tool for handling this kind of uncertainty [22]. Because fuzzy membership and probabilistic uncertainty are conceptually distinct, their combination in stochastic evolutionary games requires explicit modeling assumptions [23]. Related studies have also applied computational game theory to energy systems. Cheng et al. [24] examined evolutionary smart contracts for virtual power plant trading by integrating prospect theory

and multi-stage negotiation. Cheng et al. [25] reviewed computational game-theoretic models for adaptive urban energy systems, while Wang et al. [26] systematically reviewed evolutionary game applications in energy storage systems. Although these studies address different application contexts, they provide useful perspectives on strategic interactions and decision-making under uncertainty. Accordingly, this study focuses on three related questions: (1) Under what conditions the initial placement of greenwashing strategies across highly connected and peripheral firms influences their subsequent evolution; (2) how strategic inertia, imitation intensity, and payoff evaluation mechanisms condition evolutionary outcomes in heterogeneous networks; and (3) whether greenwashing dynamics are sensitive to different fuzzy payoff specifications and stochastic payoff sampling mechanisms.

To address these questions, this paper develops a network-based evolutionary game framework integrating a Barabási–Albert (BA) scale-free supply chain network, degree-dependent strategic inertia, triangular fuzzy payoffs, and a Fermi imitation mechanism with bounded rationality.

## 2. Literature review

### *2.1. Research on green supply chains and greenwashing behavior*

Greenwashing behavior refers to the behavior of enterprises that create a green image through false propaganda, selective disclosure, or exaggeration of their environmental contributions without taking substantive environmental actions. In the supply chain context, greenwashing behavior is more covert and may spread through interfirm relationships and strategic interactions [1,7]. Its causes are complex and can be deconstructed from multiple dimensions.

From the perspective of capital markets and financing constraints, enterprises may engage in greenwashing to obtain financial benefits, manage external perceptions, or respond to pressures associated with green transformation [4]. Green fund holdings may influence corporate greenwashing behavior, although the direction and effectiveness of this relationship depend on the governance mechanisms involved [5]. Liu et al. [27] further examined greenwashing governance in green financial products through a tripartite evolutionary game, demonstrating the relevance of interactions among financial stakeholders.

From the perspective of supply chain management and external pressure, supply chains' green gaps and customer concentration have been examined as factors associated with corporate greenwashing [2,3]. The peer effect is also an important driver of the proliferation of greenwashing. Lu et al. [6] found that corporate environmental, social, and governance (ESG) information disclosure exhibits significant industry-related and regional peer effects, while Chen et al. [7] investigated similar effects within board networks. Conversely, bank–enterprise digital coupling and corporate digital transformation have been identified as potential governance mechanisms [28,29].

From the perspective of institutional regulation and environmental regulation, governments' environmental regulation tools have a significant constraining effect on corporate greenwashing. Existing studies have examined emission permit systems, green credit interest subsidies, and digital environmental monitoring as governance mechanisms [30]. Evolutionary game analyses have likewise investigated enterprises' responses to dynamic regulation and ESG disclosure incentives [31].

From the perspective of enterprise heterogeneity and internal governance, Han [32] showed that the environmental protection background of independent directors can significantly reduce the degree of corporate greenwashing. Wang and Cao [29] pointed out that digital transformation can inhibit

corporate greenwashing by improving the quality of accounting information and alleviating financing constraints. Recent evolutionary game studies have further examined greenwashing from different stakeholder and governance perspectives. Gao et al. [1] investigated ESG greenwashing in electric vehicle supply chains, while Xue et al. [11] analyzed the evolutionary interactions among enterprises, governments, and consumers. Hao et al. [12] examined the strategic interactions among enterprises, investors, and rating agencies in ESG disclosure. Majumdar and Giri [13] investigated blockchain and big data information services for mitigating greenwashing in closed-loop supply chains. These studies highlight the importance of stakeholder interactions, regulatory mechanisms, and information-based governance. In contrast, the present study focuses on the conditional effects of the initial network position, uncertain payoff realizations, and strategic inertia on the local diffusion of greenwashing among interconnected enterprises, with particular attention to the roles of payoff accumulation and alternative behavioral specifications.

Although the aforementioned literature reveals the causes and governance paths of greenwashing from multiple perspectives, the existing models often emphasize stakeholder incentives and regulatory relationships rather than the detailed network positions of interacting enterprises. Consequently, how heterogeneous connectivity and initial strategy allocation jointly affect the diffusion of greenwashing warrants further examination.

### *2.2. Evolutionary games on supply chain networks and complex network theory*

Complex network theory provides a powerful tool for characterizing the complex interactions among enterprises in supply chains. Cui et al. [33] systematically reviewed supply chain research based on complex network methods. Barabási and Albert [14] established the preferential attachment mechanism underlying BA scale-free networks, while Santos and Pacheco [15] demonstrated that network heterogeneity can promote cooperation under specific evolutionary game conditions.

In terms of supply chain network construction methods, Ding and Chen [34] introduced antipreferential probability based on the BA network model. Zhao et al. [35] constructed a local-world evolution model for weighted complex supply chain networks, while Cao and Xiong [36] incorporated edge benefits into the network's formation. These approaches provide alternative representations of heterogeneous enterprise relationships, although their structural assumptions differ.

Applying evolutionary game theory to complex networks has become an important direction in recent years. Nowak and May [16] revealed the mechanism of network reciprocity. Szabó and Fath systematically reviewed evolutionary games on graphs [17]. In supply chain network-related evolutionary game research, Zhou and Li [18] investigated the co-evolution of information sharing and motivation, while Wu et al. [19] examined green packaging diffusion in logistics enterprise clusters. Zhang and Li [37] investigated information sharing in prefabricated building supply chains, and Wang [38] reviewed learning mechanisms in complex network evolutionary games.

More recent applications have addressed green innovation diffusion and blockchain-enabled green supply chains [20,21], while Wu et al. [39] incorporated prospect theory into complex-network evolutionary games of green technology innovation. Duan et al. [40] further investigated long-term payoff mechanisms in heterogeneous network games, providing a related perspective on the relationship between payoff evaluation and network structure.

However, these studies do not fully resolve how the initial placement of greenwashing across high- and low-degree enterprises interacts with strategic inertia, Fermi imitation, and accumulated

versus degree-normalized payoffs. The present study therefore focuses on these specific mechanisms rather than treating network heterogeneity or social learning as entirely unexplored concepts.

### *2.3. Fuzzy set theory and games under uncertainty*

In real-world decision-making environments, enterprises' perceptions of key parameters are often vague and imprecise. Fuzzy set theory provides an effective mathematical tool for handling this kind of uncertainty. Triangular fuzzy numbers, owing to their simple operation and strong intuitiveness, have become one of the most widely used forms of fuzzy number representation. Possibility theory further provides theoretical support for comparison and decision-making under fuzzy environments.

**Table 1.** Comparison of closely related studies and the present research.

| Study | Research focus | Network setting | Payoff uncertainty | Research gap |
|---|---|---|---|---|
| Gao et al. [1] Greenwashing governance | ESG greenwashing in electrical vehicle supply chains; tripartite evolutionary game | Multistakeholder interactions | No explicit fuzzy–stochastic distinction | Limited analysis of degree-based strategy placement |
| Xue et al. [11] Greenwashing governance | Dynamic greenwashing governance involving firms, governments, and consumers | Multistakeholder interactions | No triangular fuzzy payoff modeling | Limited consideration of network-based imitation |
| Yang et al. [21] Network evolutionary games | Blockchain-enabled green supply chain evolution | Complex supply chain network | No explicit fuzzy–probability distinction | Does not examine greenwashing placement or inertia |
| Wu et al. [39] Network evolutionary games | Green innovation diffusion with prospect-theoretic preferences | Heterogeneous complex networks | Prospect-theoretic preferences | Limited analysis of stochastic triangular payoffs |
| Khalil et al. [23] Stochastic network games | Cooperation dynamics using master equations and Monte Carlo simulations | Structured interaction networks | Stochastic evolutionary dynamics | Does not address supply chain greenwashing |
| Dubois and Prade [22] Fuzzy uncertainty | Theoretical distinction between possibility and probability | Not network-based | Possibility–probability distinction | Does not model network strategy diffusion |
| Present study Integrated framework | Network evolutionary model of greenwashing with inertia-modified Fermi imitation | BA networks; placement, K, N, and connectivity checks | Triangular fuzzy representation; separate stochastic payoff sampling; operator comparisons | Conditional simulation-based mechanisms; not an empirically calibrated regulatory optimum |

A key distinction is that fuzzy membership functions characterize degrees of membership or possibility, whereas probability distributions represent stochastic uncertainty [22]. Therefore,

stochastic payoff sampling in the present model is introduced through an explicitly specified probability distribution rather than by treating fuzzy membership values directly as probability densities.

Related research has investigated deterministic and stochastic cooperation transitions in evolutionary games on networks [23], while prospect theory has been incorporated into complex-network evolutionary games of green technology innovation [39].

In this study, triangular fuzzy numbers represent imprecise payoffs. Weighted defuzzification provides an analytical benchmark, whereas stochastic simulations use a specified triangular probability distribution. Because weighted defuzzification and probabilistic expectation may yield different values for asymmetric triangular specifications, this distinction is explicitly considered in the model and subsequent sensitivity analysis.

As shown in Table 1, existing studies provide complementary insights into greenwashing governance, network-based evolutionary dynamics, and uncertainty representation. The present work combines these strands while explicitly limiting its conclusions to the specified stochastic network model and numerical controls.

### *2.4. Research gaps and positioning of this paper*

On the basis of the abovementioned literature review, this paper identifies three major research gaps.

First, although research has examined greenwashing governance, peer effects, and complex network interactions, the influence of greenwashing's initial placement across firms with different connectivity levels requires further investigation. In particular, allocating an identical number of initial greenwashing strategies to high-degree, random, or low-degree enterprises may produce different evolutionary outcomes.

Second, the joint effects of degree-dependent strategic inertia, Fermi imitation intensity, and payoff accumulation mechanisms remain insufficiently understood in heterogeneous greenwashing networks. Distinguishing accumulated from degree-normalized payoffs and examining alternative inertia specifications are particularly important because network degree can influence interaction opportunities, payoff comparisons, and resistance to strategy changes simultaneously.

Third, the integration of triangular fuzzy payoffs with stochastic network evolution requires explicit treatment of the relationship among fuzzy representations, probabilistic sampling, and analytical approximations. This distinction is important for interpreting finite-horizon simulation outcomes under payoff uncertainty.

Accordingly, the present study integrates a BA scale-free network, degree-dependent inertia, triangular fuzzy payoffs, and Fermi imitation to investigate these three issues within a unified framework. It seeks to clarify the conditional effects of the initial strategy placement, behavioral mechanisms, and payoff uncertainty on the evolution of supply chain greenwashing, thereby providing a basis for more targeted governance analysis.

## 3. Model construction

### *3.1. Supply chain network topology and node heterogeneity*

#### 3.1.1. Network generation mechanism

Real-world supply chain systems are not uniform, randomly connected networks; rather, they exhibit a distinct hierarchical feature of core enterprises dominating, surrounded by numerous small

and medium-sized enterprises. This topological structure is consistent with the heterogeneous connectivity represented by BA scale-free networks [14].

***G* = (*V*, *E*) Definition 1.** Let the supply chain network be an undirected graph $G = (V, E)$, where the node set $V = \{1, 2, \ldots, N\}$ represents independent enterprises in the supply chain, and the edge set $E$ represents transaction and business relationships between enterprises. The network is generated using the BA preferential attachment model. In the baseline configuration, the network size is $N = 100$ the number of edges attached by each new node is $m = 3$, and the network-generating random seed is fixed at 42. The implementation follows the standard Network X BA generator, which takes $N$ and $m$ as its principal inputs without requiring a separately specified initial core parameter $m_0$. Figure 1 illustrates that hub nodes possess relatively high connectivity and occupy prominent positions in the network, which may provide additional opportunities for their strategies to influence local evolutionary interactions.

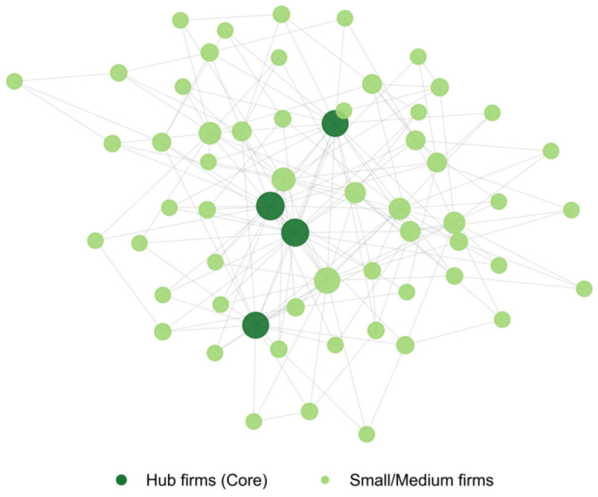



**Figure 1.** Schematic diagram of a scale-free supply chain network's topology.

**Definition 2.** The hub set $H$ consists of the $K$ highest-degree nodes in the network

$$H = \mathrm{TopK}_{i \in V}(k_i), \qquad K = 5, \tag{1}$$

where $k_i$ denotes the degree of node $i$. Thus, the hub set represents the five most highly connected enterprises in the baseline network rather than a separate category determined by strategic inertia.

In the baseline network realization, the degrees of the five hub nodes are 30, 28, 26, 23, and 23, respectively. The hub degree's share is calculated as follows:

$$W_h = \frac{\sum_{i \in H} k_i}{\sum_{i \in V} k_i} = \frac{30 + 28 + 26 + 23 + 23}{582} \approx 0.2234. \tag{2}$$

This value is specific to the realized network and should not be interpreted as a universal property of BA networks. It may vary with network size, the attachment parameter $m$, and the network's

realization. Moreover, $W_h$ represents the proportion of total node degree attributable to the hub set; it does not directly measure the probability that any particular peripheral enterprise selects a hub as its imitation target.

The degree distribution of the network can be approximately characterized by a power law distribution $P(k) \propto k^{-\beta}$, characterizing the heterogeneous structure in which a few hub nodes have high connectivity, while most nodes have relatively low degrees. For a finite network of $N = 100$, however, the use of a BA generator does not by itself establish that the realized degree distribution satisfies an exact power law.

Topological heterogeneity may influence the diffusion of greenwashing strategies by shaping enterprises' interaction opportunities, accumulated payoffs, and local imitation relationships. Although highly connected nodes interact with more neighboring enterprises, their influence on evolutionary outcomes also depends on their initial strategies, the payoff structure, and the strategy-updating mechanism. Therefore, network connectivity is treated as a potential source of heterogeneous strategic influence rather than a sufficient condition for determining the system's final state.

### 3.1.2. Degree-dependent strategic inertia

In supply chains' decision-making, enterprises may differ in their adjustment costs, organizational complexity, and the persistence of strategic choices. To represent this behavioral heterogeneity, this study assumes that enterprises with higher network connectivity exhibit greater resistance to strategy changes. This assumption is introduced as a modeling hypothesis rather than as a mathematical consequence of the BA network structure.

**Definition 3.** Each node $i \in V$ is assigned a strategic inertia coefficient $\rho_i \in [0, 1]$, which is defined as a nondecreasing function of node degree

$$\rho_i = \rho_{\min} + (\rho_{\max} - \rho_{\min}) \frac{k_i}{k_{\max}}, \tag{3}$$

where $\rho_{min}$ and $\rho_{max}$ represent the lower and upper parameter bounds of strategic inertia, respectively, and $k_{max}$ denotes the maximum degree in the network.

It should be noted that $\rho_{min}$ is a lower bound parameter of the inertia function rather than necessarily the minimum inertia realized in the network. Because the baseline BA network contains no isolated nodes and $k_{min} > 0$, the minimum realized inertia satisfies

$$\min_{i \in V} \rho_i = \rho_{\min} + (\rho_{\max} - \rho_{\min}) \frac{k_{\min}}{k_{\max}} > \rho_{\min}, \tag{4}$$

provided that $\rho_{max} > \rho_{min}$. In contrast, the node with the maximum degree attains the upper-bound value $\rho_{max}$.

The assumed positive relationship between the node degree and strategic inertia reflects a stylized behavioral mechanism: Enterprises occupying more highly connected positions may face greater coordination requirements and adjustment costs when changing established strategies. This relationship is not assumed to hold universally across real-world supply chains. Instead, its implications are examined through the subsequent sensitivity analysis.

The degree-dependent inertia function is maintained in the baseline model and in experiments that do not explicitly vary the inertia mechanism. Alternative inertia specifications, including constant, reverse-

degree, random, and zero-inertia settings, are examined separately in the robustness and mechanism ablation experiments. In the inertia sensitivity experiment, different inertia configurations are constructed by varying $\rho_{min}$ and $\rho_{max}$, while preserving the same degree-dependent functional relationship.

Finally, the hub's classification and strategic inertia should be distinguished. The hub set $H$ is a discrete group determined by the degree ranking and is used primarily for the initial strategy allocation and group-based comparisons. In contrast, strategic inertia is a continuously degree-dependent node attribute assigned to every enterprise and is incorporated into the strategy-updating probability. Although both depend on the network degree, they serve different purposes in the model.

### *3.2. Fuzzy game payoff matrix and defuzzification*

#### 3.2.1. Construction of triangular fuzzy numbers

In real-world supply chain games, enterprises' perceptions of the key payoff parameters may be vague or imprecise due to market fluctuations, policy uncertainty, and information asymmetry. Triangular fuzzy numbers are therefore introduced to represent imprecise payoff information, drawing on the distinction between possibility and probability discussed by Dubois and Prade [22]. This paper introduces triangular fuzzy numbers to describe this decision-making uncertainty.

**Definition 4.** For any fuzzy payoff variable, the triangular fuzzy number corresponding to its membership function is defined as $\tilde{X} = (X^p, X^r, X^o)$, where $X^p$ represents the pessimistic value, $X^r$ represents the realistic (most likely) value, and $X^o$ represents the optimistic value. This three-value representation provides a tractable description of imprecise payoff bounds for subsequent analytical comparisons and stochastic evolutionary simulations.

#### 3.2.2. Strategy space and payoff matrix

Each enterprise $i$ in the supply chain has a pure strategy space $W = \{G, B\}$, where $G$ denotes the adoption of a genuine green production strategy, and $B$ denotes the adoption of a greenwashing strategy. Following the classical game-theoretic framework, this paper defines the fuzzy payoff matrix when enterprise $i$ engages in a bilateral game with its neighbor $j$. The fuzzy payoff parameters defined in Table 2.

**Table 2.** Payoff matrix of the two-strategy supply chain evolutionary game.

| Focal enterprise *i* / neighbor *j* | Genuine green (*G*) | Greenwashing (*B*) |
|---|---|---|
| Genuine green (*G*) | $\tilde{R}$ | $\tilde{S}$ |
| Greenwashing (*B*) | $\tilde{T}$ | $\tilde{P}$ |

In Table 2, $\tilde{R}$ represents the mutual benefits of genuine green cooperation, including potential reputational advantages and green financing incentives. The payoff $\tilde{S}$ denotes the losses experienced by a genuinely green enterprise when its counterpart engages in greenwashing. The payoff $\tilde{T}$ represents the potential speculative gains obtained through greenwashing when the neighboring enterprise adopts genuine green production. Finally, $\tilde{P}$ captures the net losses associated with mutual greenwashing, including potential reputational damage and regulatory penalties.

Under the baseline accumulated payoff mechanism, the total payoff of enterprise $i$ at time $t$ is

$$\Pi_i(t) = \sum_{j \in N_i} a_{s_i(t), s_j(t)}(t), \tag{5}$$

where $N_i$ denotes the neighbor set of the node $i$, and $a_{s_i(t),s_j(t)}(t)$ denotes the realized payoff associated with the corresponding strategy combination. The accumulated payoff mechanism is used in the baseline model; degree-normalized payoffs are considered as an alternative specification in the robustness analysis.

### 3.2.3. Weighted defuzzification and stochastic payoff sampling

For the deterministic mean-field analysis, this study uses a weighted defuzzification operator to convert triangular fuzzy payoff representations into scalar reference values. The resulting values are used exclusively to characterize the analytical payoff structure and should not be interpreted as probabilistic expectations or formally derived fuzzy equilibrium payoffs.

**Definition 5.** For any triangular fuzzy number $\tilde{X} = (X^p, X^r, X^o)$, its weighted defuzzified value is defined as

$$D_w(\tilde{X}) = \frac{X^p + 2X^r + X^o}{4} \tag{6}$$

The operator places greater weight on the modal value $X^r$ and provides a deterministic scalar representation of the fuzzy payoff for the analytical framework. It is a defuzzification convention rather than the probabilistic expectation of a triangular random variable.

Two distinct forms of uncertainty are considered in the numerical framework. The first is parameter uncertainty, represented by the triangular fuzzy payoff specifications $\tilde{X} = X^p, X^r, X^o$. These specifications describe imprecise payoff information through pessimistic, modal, and optimistic values, without assigning probability measures to the fuzzy membership grades.

The second is interaction-level stochasticity, which concerns the realization of bilateral payoffs during local strategic interactions. To operationalize this stochastic component, an additional triangular probability distribution is explicitly assumed to share the same lower bound, mode, and upper bound as the corresponding fuzzy payoff specification. This distribution is not derived from the fuzzy membership function; rather, it constitutes a separate stochastic modeling assumption.

Under the baseline comparison-level sampling mechanism, a new payoff realization is independently generated for each bilateral interaction whenever the accumulated payoff of a focal firm or its selected neighbor is evaluated. Consequently, the resulting payoff differences reflect both the firms' current strategy configurations and stochastic variation in the local interaction outcomes. Specifically, the realized bilateral payoff is sampled as follows:

$$X \sim \text{Triangular}(X^p, X^r, X^o). \tag{7}$$

The expected value of the triangular probability distribution is

$$\text{E}[\tilde{X}] = \frac{X^p + X^r + X^o}{3}. \tag{8}$$

Therefore, the weighted defuzzified value and the probabilistic expectation may differ for asymmetric triangular specifications. The theoretical benchmark and stochastic simulations are treated as distinct payoff representations, and their results are not assumed to coincide.

### *3.3. Social learning and asynchronous updating based on bounded rationality*

In real-world supply chains, enterprises do not possess global optimal decision-making capabilities. This paper adopts an asynchronous updating mechanism to represent decentralized, bounded, rational strategy adjustments among interconnected enterprises and to examine their consequences for greenwashing evolution.

At each time step, a fraction $\lambda = 0.2$ of the $N$ enterprises is randomly selected without replacement for sequential strategy updating. The selected enterprises are processed in random order, and each update takes effect immediately before the next enterprise is processed. For each selected enterprise $i$, the updating procedure is defined as follows.

(i) Local comparison: Randomly select a neighbor $j \in N_i$ as the learning benchmark. If $s_i(t) = s_j(t)$, no strategy change is considered. Otherwise, the accumulated payoffs $\Pi_i(t)$ and $\Pi_j(t)$ are independently recalculated by sampling the payoff of every neighboring interaction according to the corresponding strategy combination, using the stochastic payoff mechanism specified in Section 3.2.3.

(ii) Payoff difference: Calculate $\Delta\Pi_{ij}(t) = \Pi_j(t) - \Pi_i(t)$. Unlike an improvement-only imitation rule, the updating procedure does not require $\Delta\Pi_{ij}(t) > 0$.

(iii) Imitation probability: Node $i$ adopts the strategy of neighbor $j$ with probability $P_{i\leftarrow j}(t)$, given by the inertia-modified Fermi rule

$$P_{i\leftarrow j}(t) = \frac{1-\rho_i}{1+\exp[-\eta(\Pi_j(t)-\Pi_i(t))]}, \tag{9}$$

where $\eta$ is the social learning intensity, representing the enterprise's sensitivity to external payoff differences. The parameter $\rho_i$ reduces the probability of strategy switching, with $1 - \rho_i$ representing its upper bound. When $\eta \to 0$, the imitation probability approaches $1 - \rho_i / 2$ for different strategies. As $\eta \to \infty$, the probability approaches $1 - \rho_i$ for positive payoff differences and zero for negative differences; when payoffs are equal, it remains $1 - \rho_i / 2$.

### *3.4. System evolutionary dynamics measurement and convergence criteria*

To quantify the degree of diffusion and the evolutionary process of greenwashing behavior in the supply chain network, this paper defines the global macro-state indicators.

**Definition 6.** At time $t$, the proportion of enterprises in the network adopting the greenwashing strategy $B$ is defined as the greenwashing density $f(t)$

$$f(t) = \frac{1}{N}\sum_{i=1}^{N}\mathbf{1}\{s_i(t) = B\}, \tag{10}$$

where $1\{\cdot\}$ is the indicator function. The value $f(t) = 0$ corresponds to the all-green state, and $f(t) = 1$ corresponds to the all-greenwashing state.

The global density $f(t)$ is used as the primary evolutionary outcome. Although it does not distinguish enterprises by network connectivity, it directly measures the proportion of greenwashing

enterprises and remains valid for heterogeneous networks. To examine the structural differences, hub strategies and degree-related characteristics are analyzed separately rather than incorporated into an assumed weighted diffusion probability.

To assess the stability of simulated trajectories, a quasi-convergence diagnostic is defined as

$$\sigma_L(t) = \mathrm{Std}\left[f(t-L+1),\ldots,f(t)\right] < \delta, \tag{11}$$

where $L = 20$ is the observation window's length and $\delta = 0.005$ is the specified fluctuation threshold. The first time this condition is satisfied is recorded as the quasi-convergence time. This criterion indicates low short-term variation in the greenwashing density but does not establish an absorbing state or asymptotic stability.

The simulation is conducted over a fixed horizon of $T = 1000$ time steps without early termination. The terminal greenwashing density is defined as $f(T)$. A homogeneous absorbing state is identified when $f(t) \in \{0, 1\}$, corresponding to all-green or all-greenwashing strategies, respectively. Simulations that do not reach either absorbing state by $T$ are classified as nonabsorbed within the observation horizon, rather than as having necessarily converged to a stable mixed equilibrium.

The absorption time is defined as $\tau_{abs} = inf\{t: f(t) \in \{0,1\}\}$, with $\tau_{\mathrm{abs}} = \infty$ recorded if the system does not reach a homogeneous absorbing state by $T$. In repeated simulations, runs with $\tau_{\mathrm{abs}} = \infty$ are treated as right-censored when computing the mean absorption times.

To account for stochastic variability, the numerical experiments use repeated Monte Carlo simulations and summarize evolutionary outcomes using the mean trajectories, terminal greenwashing densities, and uncertainty estimates.

## 4. Model analysis

### *4.1. Mean-field approximation and equilibrium stability*

When studying evolutionary games in structured populations, traditional mean-field theory typically assumes that all nodes in the network are homogeneous, i.e., individuals are randomly mixed, ignoring topological structural differences. Based on the payoff matrix defined in Chapter 3, let $f$ denote the proportion of nodes adopting the greenwashing strategy $B$, i.e., the global greenwashing density $f(t)$. According to mean-field theory, when a node randomly encounters a peer, the probability of encountering a greenwashing node is $f$, and the probability of encountering a true green node is $1 - f$.

Thus, the expected per-interaction payoffs of adopting the greenwashing strategy $B$ and the genuine green strategy $G$ can be expressed as

$$\pi_B(f) = (1-f)T + fP, \tag{12}$$

$$\pi_G(f) = (1-f)R + fS. \tag{13}$$

Define the expected payoff difference as $\Delta(f) = \pi_B(f) - \pi_G(f)$. Expanding and rearranging yields

$$\Delta(f) = (T-R) + f[(P-T)-(S-R)]. \tag{14}$$

According to the replicator dynamics equation of evolutionary games, the corresponding homogeneous mean-field dynamics are

$$\dot{f} = f(1-f)\Delta(f). \tag{15}$$

An interior equilibrium exists when $\Delta(f^*) = 0$ and $0 < f^* < 1$, giving

$$f^* = \frac{T-R}{(T-R)+(S-P)}. \tag{16}$$

Under the baseline defuzzified payoff parameters $R = 0.12$, $S = -0.02$, $T = 0.20$, and $P = -0.03$, the payoff difference becomes $\Delta(f) = 0.08 - 0.09f$ and the interior equilibrium is $f^* = 0.08 / 0.09 \approx 0.8889$.

Since $\Delta(f) > 0$ for $0 < f < f^*$ and $\Delta(f) < 0$ for $f^* < f < 1$, the replicator dynamics satisfy $\dot{f} > 0$ below $f^*$ and $\dot{f} < 0$ above $f^*$. Consequently, $f^*$ is an asymptotically stable interior equilibrium of the homogeneous replicator model, whereas the boundary equilibria $f = 0$ and $f = 1$ are unstable under the baseline payoff configuration.

Importantly, this result does not imply that the stochastic BA network converges to $f^* = 0.8889$. The mean-field model assumes homogeneous interactions and deterministic payoffs, whereas the network simulations incorporate heterogeneous connectivity, degree-dependent inertia, stochastic payoffs, and local Fermi imitation. Therefore, $f^*$ serves as an analytical reference for understanding the relative strategic incentives rather than an exact prediction of finite-network terminal outcomes or a tipping threshold separating all-green and all-greenwashing absorbing states.

### *4.2. Effects of topological heterogeneity on local interactions*

Real-world supply chain networks, especially BA scale-free networks, are not homogeneous networks. Their heterogeneous degree distributions imply that enterprises differ in the number of interaction partners and opportunities for local strategy imitation. In heterogeneous networks, the global greenwashing density *f(t)* is no longer the sole variable determining the system's subsequent evolutionary dynamics. The nodes' strategy updates depend on their direct game payoffs with local neighbors.

For an enterprise $i$ with degree $k_i$, define its local greenwashing exposure as

$$q_i(t) = \frac{1}{k_i} \sum_{j \in N_i} \mathbf{1}\{s_j(t) = B\}, \tag{17}$$

The local exposure measure $q_i(t)$ should be distinguished from the global greenwashing density $f(t)$, as well as the group-level densities $f_H(t)$ and $f_p(t)$. It describes the strategy composition of node *I*'s immediate neighborhood and does not incorporate degree-based weighting across the entire network.

Under the accumulated-payoff mechanism defined in Section 3.2, the expected payoff of enterprise *i*, conditional on its current strategy and its neighbors' strategies, can be expressed as

$$\mathrm{E}[\Pi_i(t) \mid s_i(t) = G, q_i(t)] = k_i[(1-q_i(t))\bar{R} + q_i(t)\bar{S}], \tag{18}$$

$$\mathrm{E}[\Pi_i(t) \mid s_i(t) = B, q_i(t)] = k_i[(1-q_i(t))\bar{T} + q_i(t)\bar{P}], \tag{19}$$

where $(\bar{R}, \bar{S}, \bar{T}, \bar{P})$ denote the probabilistic expectations of the corresponding stochastic payoff distributions. For the symmetric baseline triangular specifications, these expectations coincide with the weighted defuzzified values used in Section 4.1.

Eq (18) and Eq (19) show that the expected accumulated payoffs depend jointly on the node degree and local strategy composition. Although highly connected enterprises participate in more interactions, a larger degree does not necessarily imply a higher realized payoff or greater imitation success.

Because the imitation target is selected uniformly from the focal enterprise's neighbors, the probability that node $i$ selects a hub node is

$$P(j \in H \mid i) = \frac{|N_i \cap H|}{k_i}. \tag{20}$$

This local probability differs from the aggregate hub degree share $W_h$ = 0.2234 reported in Section 3.1. The latter measures the hubs' contribution to total network degree and cannot be directly substituted for individual neighbor selection probabilities.

Consequently, the evolutionary influence of hub nodes depends on their actual connections, initial strategies, accumulated payoffs, and degree-dependent inertia. Network topology shapes the opportunities and incentives for a strategy's diffusion but does not independently determine whether the finite network reaches an all-green or all-greenwashing absorbing state.

### *4.3. Conditional influence of hub strategy placement*

In heterogeneous supply chain networks, hub nodes may influence greenwashing diffusion through their connectivity, initial strategy choices, and strategic inertia. However, their influence is conditional rather than sufficient to determine the network's final evolutionary state.

To characterize the initial distribution of greenwashing strategies among highly connected enterprises, define the hub greenwashing density as

$$f_H(t) = \frac{1}{|H|} \sum_{i \in H} \mathbf{1}\{s_i(t) = B\}. \tag{21}$$

Similarly, the greenwashing density among peripheral enterprises is

$$f_P(t) = \frac{1}{N - |H|} \sum_{i \in P} \mathbf{1}\{s_i(t) = B\}. \tag{22}$$

These quantities describe strategy composition within different network groups, while the global greenwashing density satisfies

$$f(t) = \frac{|H|}{N} f_H(t) + \frac{N - |H|}{N} f_P(t). \tag{23}$$

The potential influence of hub strategies can be understood through three interacting mechanisms. First, highly connected enterprises participate in more bilateral interactions, affecting the number of local contacts through which their strategies may be observed. Second, under accumulated payoffs, network degree contributes to differences in total payoff magnitudes, although the direction of the resulting payoff advantage depends on the strategies of neighboring enterprises. Third, the degree-dependent inertia mechanism reduces the probability that highly connected enterprises change their existing strategies, potentially increasing the persistence of their initial choices.

These mechanisms do not imply that hub strategies determine network-wide outcomes. In particular, the probability that a peripheral enterprise selects a hub as an imitation target depends on

its actual neighborhood, as defined in Eq (20), rather than the aggregate hub degree share. Moreover, imitation remains stochastic and depends on the local payoff differences.

Accordingly, the initial placement of greenwashing strategies may influence finite-horizon evolutionary outcomes even when the initial number of greenwashing enterprises is held constant. This motivates a comparison of high-degree, randomly selected, and low-degree initial placements, together with alternative hub strategy configurations in the numerical experiments.

The purpose of this analysis is therefore to identify the conditions under which the network position amplifies or attenuates greenwashing diffusion, rather than to establish an unconditional hub anchoring effect or a universal threshold for all-green or all-greenwashing convergence.

### *4.4. Sensitivity of evolutionary incentives to fuzzy payoffs*

Traditional mean-field theory relies on precise expected value calculations. However, in fuzzy payoff environments, uncertainty in the payoff parameters may affect both the expected strategic incentives and the stochastic evolutionary outcomes. This section examines how changes in the optimistic bound of greenwashing temptation $T^o$ and the pessimistic bound of genuine green cooperation $R^p$ influence the difference in payoff under the weighted defuzzification framework.

Substituting the defuzzified payoffs defined in Section 3.2 into Eq (15), the homogeneous mean-field payoff difference becomes

$$\Delta(f) = (1-f)\left[D_w(\tilde{T}) - D_w(\tilde{R})\right] + f\left[D_w(\tilde{P}) - D_w(\tilde{S})\right]. \tag{24}$$

For an interior equilibrium satisfying $0 < f^* < 1$, its location is

$$f^* = \frac{D_w(\tilde{T}) - D_w(\tilde{R})}{D_w(\tilde{T}) - D_w(\tilde{R}) + D_w(\tilde{S}) - D_w(\tilde{P})}. \tag{25}$$

Using the weighted defuzzification operator $D_w(\tilde{X}) = (X^p + 2X^r + X^o)/4$, the sensitivity of the payoff difference to the optimistic bound of greenwashing temptation is

$$\frac{\partial \Delta}{\partial T^o} = \frac{1-f}{4} \geq 0. \tag{26}$$

Similarly, the sensitivity to the pessimistic genuine green payoff bound is

$$\frac{\partial \Delta}{\partial R^p} = -\frac{1-f}{4} \leq 0. \tag{27}$$

These derivatives are calculated while holding the other payoff parameters and the greenwashing density $f$ fixed. They indicate that increasing $T^o$ strengthens the relative payoff incentive for greenwashing, whereas increasing $R^p$ weakens it, under the homogeneous deterministic approximation. Both sensitivities become zero at $f = 1$, where all interactions occur between greenwashing enterprises.

However, adjusting the bounds of a triangular payoff representation may also change the probabilistic expectation and dispersion of the stochastic payoff distribution used in the numerical simulations. Under the assumed triangular probability distribution, $\mathbb{E}[\tilde{X}] = (X^p + X^r + X^o)/3$, which generally differs from the weighted defuzzified value for asymmetric triangular specifications.

Consequently, Eq (26) and Eq (27) characterize changes in the analytical payoff incentives rather than sufficient conditions for convergence to either homogeneous absorbing state in the stochastic BA

network. The numerical experiments therefore distinguish extreme boundary adjustments, which also alter central payoff values, from mean-controlled changes in payoff interval widths.

From a governance perspective, reducing the upper bound of speculative greenwashing returns or strengthening the lower bound of genuine green returns may shift relative strategic incentives toward genuine green production. However, the consequences for finite-horizon greenwashing density remain conditional on network connectivity, initial strategy placement, strategic inertia, and stochastic imitation.

### *4.5. Interactive effects of social learning intensity and strategic inertia*

In heterogeneous networks, the diffusion of strategies among nodes relies on the social learning mechanism. According to the modified Fermi rule defined in Chapter 3, the probability that node $i$ imitates node $j$ after comparing payoffs is

$$P_{i\leftarrow j}=\frac{1-\rho_i}{1+\exp[-\eta(\Pi_j-\Pi_i)]}. \tag{28}$$

Let $\Delta\Pi_{ij}=\Pi_j-\Pi_i$. The effects of social learning intensity $\eta$ and strategic inertia $\rho_i$ on the imitation probability can be examined through their partial derivatives as follows:

$$\frac{\partial P_{i\leftarrow j}}{\partial\eta}=(1-\rho_i)\Delta\Pi_{ij}\frac{\exp(-\eta\Delta\Pi_{ij})}{[1+\exp(-\eta\Delta\Pi_{ij})]^2}, \tag{29}$$

$$\frac{\partial P_{i\leftarrow j}}{\partial\rho_i}=-\frac{1}{1+\exp(-\eta\Delta\Pi_{ij})}<0. \tag{30}$$

These derivatives are evaluated for fixed payoff differences and other model parameters. Eq (29) indicates that increasing social learning intensity raises the probability of imitation when the selected neighbor has a higher payoff ($\Delta\Pi_{ij}>0$), but reduces it when the neighbor has a lower payoff ($\Delta\Pi_{ij}<0$). When the two payoffs are equal, learning intensity does not affect the imitation probability. Eq (30) shows that greater strategic inertia consistently lowers the switching probability for a given payoff difference.

Two limiting cases further illustrate these mechanisms. When $\eta\to 0$, payoff differences have little influence on imitation, and

$$\lim_{\eta\to 0}P_{i\leftarrow j}=\frac{1-\rho_i}{2}. \tag{31}$$

When $\eta\to\infty$, the updating probability approaches

$$P_{i\leftarrow j}\to\begin{cases}1-\rho_i, & \Delta\Pi_{ij}>0,\\ (1-\rho_i)/2, & \Delta\Pi_{ij}=0,\\ 0, & \Delta\Pi_{ij}<0.\end{cases} \tag{32}$$

Thus, even under strong payoff sensitivity, the maximum switching probability is constrained by strategic inertia. Moreover, a higher learning intensity does not necessarily favor genuine green strategies, because its effect depends on the strategy and relative payoff of the selected neighbor.

Through the degree-dependent inertia mechanism, highly connected enterprises are assigned greater resistance to strategy changes. This may increase the persistence of their existing strategies,

but it does not imply irreversible lock-in. Consequently, the combined effects of learning intensity, strategic inertia, and network position on the diffusion of greenwashing remain conditional on local payoff differences and the evolving strategy distribution. Their network-level implications are examined through sensitivity experiments in Chapter 5.

## 5. Numerical simulation

### *5.1. Simulation background and parameter calibration*

#### 5.1.1. Illustrative industry context and network configuration

The new energy vehicle power battery supply chain provides an illustrative context for examining greenwashing behavior in the networks of interconnected enterprises. The industry involves battery manufacturers, vehicle producers, and multiple tiers of material and component suppliers. Differences in enterprises' business relationships and connectivity motivate the use of a heterogeneous network representation. Environmental information disclosure, carbon footprint reporting, and green supply chain requirements also provide relevant contexts for examining the incentives associated with genuine green practices and greenwashing.

However, the present study does not reconstruct an empirical transaction network of power battery enterprises. Instead, a BA scale-free network is used as a stylized representation of heterogeneous supply chain connectivity. Therefore, the simulated network should not be interpreted as evidence that the actual power battery supply chain follows a BA degree distribution.

The network size is $N = 100$, and the attachment parameter is $m = 3$, with the network-generating random seed fixed at 42. As defined in Section 3.1, the five nodes with the highest degree are identified as the hub set, with degrees of 30, 28, 26, 23, and 23. Their aggregate degree share is $W_h = 0.2234$. The initial network state is set as follows: Among the five hub nodes with the highest degree, two adopt the greenwashing strategy and three adopt the genuine green strategy; the initial greenwashing ratio of peripheral nodes is 30%.

The 30% peripheral greenwashing ratio is an illustrative baseline assumption rather than an empirically estimated industry prevalence rate. To examine the dependence of the results on this assumption, Experiment 6 considers alternative initial ratios of 10%, 30%, 50%, and 70%**.**

Accordingly, the purpose of the simulations is to investigate evolutionary mechanisms under controlled network and payoff conditions, rather than to predict the actual prevalence of greenwashing among power battery supply chain enterprises.

#### 5.1.2. Payoff matrix and fuzzy interval calibration

The payoff parameters are specified to represent stylized economic incentives associated with genuine green production and greenwashing in supply chain interactions. Because firm-level bilateral transaction payoffs and the economic consequences of greenwashing are difficult to observe directly, the present study does not undertake empirical parameter estimation or calibration. Instead, normalized, dimensionless payoff values are assigned to characterize differences in strategic incentives under controlled simulation conditions.

Four payoff components are considered. The mutual green cooperation payoff $R$ represents the potential benefits of genuine green collaboration, including reputational advantages and access to

green financing. The sucker's payoff $S$ captures the disadvantage experienced by a genuinely green enterprise when interacting with a greenwashing counterpart. The temptation payoff $T$ represents potential short-term gains from greenwashing when the neighboring enterprise adopts genuine green production. The mutual greenwashing payoff $P$ represents the net consequences of interactions between two greenwashing enterprises, including potential reputational and regulatory costs.

The baseline deterministic reference payoffs are specified as $R = 0.12$, $S = -0.02$, $T = 0.20$, and $P = -0.03$. These values are illustrative assumptions rather than estimates obtained from observed financial statements, policy subsidy amounts, or transaction contracts. They represent a payoff configuration in which unilateral greenwashing yields the highest individual payoff, while mutual greenwashing produces a negative payoff.

To incorporate uncertainty, each payoff is represented by a triangular fuzzy number. The baseline specifications are reported in Table 3. The model values correspond to the deterministic reference payoffs, while the interval bounds represent alternative payoff realizations around these values. The interval widths are selected for numerical experimentation rather than calibrated from empirical probability distributions.

Under the baseline symmetric triangular specifications, weighted defuzzification and the probabilistic expectation of triangular sampling produce identical central payoff values. Asymmetric and alternative interval configurations are subsequently examined to assess the sensitivity to payoff bounds and the choice of payoff representation.

Consequently, the quantitative results should be interpreted as conditional simulation outcomes. Their purpose is to identify how network structure, behavioral mechanisms, and payoff assumptions influence greenwashing's evolution, rather than to estimate the actual monetary returns of greenwashing in the power battery industry.

**Table 3.** Triangular fuzzy payoff parameter settings under the baseline scenario.

| Fuzzy payoff parameter | Triangular fuzzy number | Illustrative modeling assumptions |
|---|---|---|
| Synergy payoff $R$ | (0.08, 0.12, 0.16) | Green credit and carbon credit returns are moderate |
| Sunk loss $S$ | (−0.04, −0.02, 0.00) | True green parties suffer reputational damage due to greenwashing's spillover |
| Short-term temptation $T$ | (0.14, 0.20, 0.26) | Huge windfall window brought by speculation |
| Double-loss penalty $P$ | (−0.06, −0.03, 0.00) | Administrative penalties and market reputation collapse after fraud exposure |

The interval width of the triangular fuzzy number, $D = X^o - X^p$, reflects the degree of certainty in policy regulation. Specifically, this is as follows.

The interval for $R$ is relatively narrow ($D$ = 0.08): Domestic green credit benchmark interest rates, carbon emission reduction support tools, and other financial policies possess strong continuity and stability.

The interval for $T$ is relatively wide ($D$ = 0.12): Greenwashing speculative returns depend strongly on the length of the regulatory "window period". The more ambiguous the policy, the greater the fluctuation in speculative space.

The interval fluctuations for $S$ and $P$: These are mainly derived from the unpredictability of "campaign-style enforcement" in environmental regulation and fluctuations in consumer sentiment.

### 5.1.3. Illustrative nature and sensitivity strategy

Given the illustrative nature of the network and payoff parameters, the robustness of the simulation findings is examined through systematic sensitivity analyses. These analyses evaluate whether the observed evolutionary patterns depend on specific baseline assumptions rather than establishing empirical representativeness.

The experiments investigate changes in the triangular payoff interval widths, extreme payoff bounds, defuzzification operators, social learning intensity, strategic inertia, the BA network's attachment parameters, the initial strategy placement, payoff accumulation rules, and initial greenwashing proportions. Where appropriate, additional control settings are used to distinguish changes in payoff expectations from changes in uncertainty and to separate network position effects from payoff evaluation effects.

All reported findings are interpreted within the tested parameter ranges and simulation horizon. Statistical nonsignificance is treated as insufficient evidence of a difference rather than proof that two mechanisms or configurations are equivalent. The detailed experimental settings and results are presented in Sections 5.2–5.7.

### 5.1.4. Simulation procedure, statistical inference, and reproducibility

To ensure the reproducibility of the numerical experiments, this study specifies the network generation procedure, stochastic updating algorithm, random seed management, and statistical inference methods. All simulations are implemented in Python using NetworkX, NumPy, and SciPy, while Matplotlib is used for visualization.

The baseline supply chain network is generated using the BA preferential attachment model through 'networkx.barabasi_albert_graph $(N, m, seed)$', with $N = 100$ and $m = 3$. The network is undirected, unweighted, and fixed throughout each simulation run. The five nodes with the highest degrees are identified as hub enterprises. The baseline initialization assigns two hub nodes to greenwashing and three to genuine green production, while 30% of peripheral enterprises initially adopt greenwashing. Alternative network parameters, hub configurations, and initial strategy allocations are examined in the corresponding sensitivity experiments.

The evolutionary process follows the asynchronous inertia-modified Fermi imitation mechanism described in Section 3. At each time step, 20% of the enterprises are selected without replacement and updated sequentially in randomized order. Each selected enterprise randomly chooses one neighboring enterprise for comparison. If their strategies differ, their payoffs are evaluated according to the specified payoff aggregation and stochastic sampling mechanisms. The focal enterprise then adopts the neighbor's strategy with the probability defined by the inertia-modified Fermi rule. Any strategy change takes effect immediately, and the global greenwashing density is recorded after the updating process. The complete simulation procedure, including BA network generation, strategy initialization, stochastic payoff evaluation, and asynchronous Fermi updating, is presented in Algorithm A1 in Appendix A. The baseline parameters and experiment-specific configurations are summarized in Table A1.

A root random seed of 42 is used to initialize reproducible simulations. The independent network realizations, initial strategy configurations, and stochastic evolutionary updates are generated using recorded random seed settings. Within paired experimental comparisons, corresponding conditions share the same network realization and matched initialization procedure.

The complete seed-generation rules and experimental configurations are documented in the accompanying source code and metadata files.

Experiment 1 uses a fixed BA network with 20 matched Monte Carlo replicates. Experiments 2–6 have 20 independently generated BA networks, with 20 Monte Carlo replicates per network and experimental condition. Each simulation is conducted for 1000 evolutionary time steps. The principal outcomes include the global greenwashing density, terminal strategy distribution, quasi-convergence diagnostics, and homogeneous absorbing-state outcomes.

For Experiments 2–6, statistical inference is performed using independent network-level means. The 20 Monte Carlo outcomes within each network are first averaged, yielding one observation per independent network. The overall mean and its two-sided 95% confidence interval are then calculated across the 20 network-level means using Student's $t$ distribution with 19 degrees of freedom. Confidence bands for the evolutionary trajectories are constructed using the same procedure at each recorded time step. For Experiment 1, confidence intervals are calculated across Monte Carlo replicates, conditional on the fixed network's realization.

Formally, let $\bar{f}_a$ denote the mean terminal greenwashing density of the 20 Monte Carlo replicates in a network $a$ as follows: $\bar{f}_a = 1/20 \sum_{r=1}^{20} f_{a,r}(1000)$, $\bar{f} = 1/20 \sum_{a=1}^{20} \bar{f}_a$.

The two-sided 95% confidence interval is calculated as $CI_{95\%} = \bar{f} \pm t_{0.975,19} \frac{s_{net}}{\sqrt{20}}$, where $s_{net}$ is the sample standard deviation of the 20 network-level means. This interval is a two-sided Student's $t$ interval based on independent network-level means; it is neither a percentile bootstrap interval nor an interval computed directly from all 400 Monte Carlo runs.

For matched comparisons involving multiple experimental conditions, Friedman tests are used to assess overall differences. Paired Wilcoxon signed-rank tests with Holm adjustment are used for subsequent pairwise comparisons. Runs that do not reach either homogeneous absorbing state within the 1000-step observation horizon are classified as nonabsorbed and treated as right-censored in the absorption time analysis. Quasi-convergence and absorption are reported as distinct outcomes.

The baseline parameters are summarized in Supplementary Table S1. Experimental configurations, simulation scripts, random seed records, and numerical results are retained to support independent verification. Information on the availability of the source code and output data is provided in the Data and Code Availability statement.

### *5.2. Experiment 1: The effect of the hub nodes' initial strategies on the system's final state*

#### 5.2.1. Experimental setup

Experiment 1 examines how the initial strategies of highly connected hub firms influence greenwashing evolution in a heterogeneous supply chain network. The experiment uses a BA scale-free network with $N = 100$ and $m = 3$, where the five nodes with the highest degree are identified as hub firms. The payoff parameters, degree-dependent strategic inertia, and asynchronous Fermi imitation mechanism follow the baseline specifications described in Section 5.1.

The three scenarios are defined as follows.

Scenario A: All five hub nodes have their initial strategies locked to green ($G$), and the peripheral nodes randomly select greenwashing with a 30% probability.

Scenario B: All five hub nodes have their initial strategies locked to greenwashing ($B$), and the peripheral nodes randomly select greenwashing with a 30% probability.

Scenario C: Among the top five hub nodes sorted by degree, the three hub nodes with the highest degrees are initially green, and the remaining two hub nodes are initially greenwashing; the peripheral nodes still randomly select greenwashing with a 30% probability. This setting simulates a transitional scenario in the real-world supply chain where the leading core enterprise group exhibits preliminary strategic divergence.

### 5.2.2. Evolutionary curve comparison analysis

Figure 2 illustrates the evolution of the global greenwashing density $f(t)$ under the three initial hub strategy scenarios. The evolutionary trajectories exhibit distinct patterns, indicating that the initial strategies of highly connected firms can influence the subsequent diffusion of greenwashing.

Under Scenario A, the mean greenwashing density initially decreases and subsequently rises gradually. The terminal mean reaches 0.4320, with a 95% confidence interval of [0.2014, 0.6626]. This indicates that initially green hub firms are associated with a lower terminal greenwashing density than in the other scenarios, although they do not necessarily prevent the subsequent spread of greenwashing.

Under Scenario B, the greenwashing density increases rapidly during the early stages of evolution and remains close to complete greenwashing adoption. The mean terminal density reaches 0.9675, with a 95% confidence interval of [0.8995, 1.0000]. This suggests that initially greenwashing hub firms can facilitate widespread diffusion under the specified network and behavioral conditions.

Scenario C exhibits an intermediate evolutionary pattern, with a terminal mean greenwashing density of 0.7195 and a 95% confidence interval of [0.5251, 0.9139]. Its comparatively broad confidence interval reflects substantial variation across Monte Carlo replicates, suggesting that mixed initial hub strategies can lead to heterogeneous evolutionary outcomes.

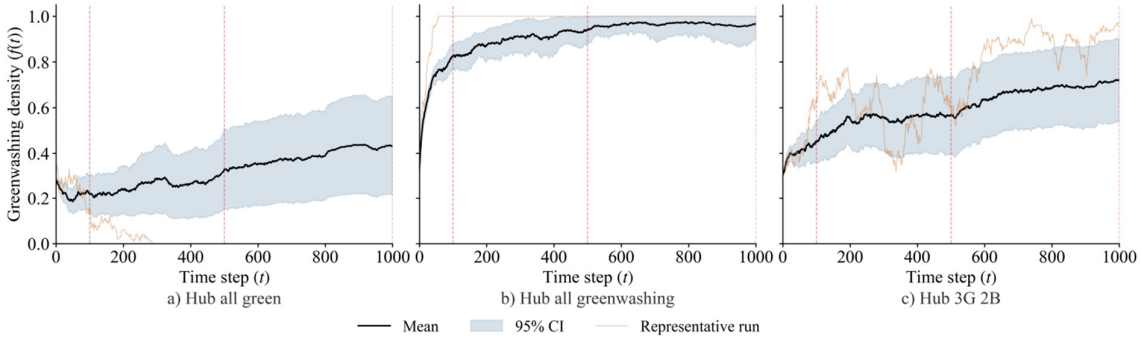



**Figure 2.** Impact of hub nodes' initial strategies on the evolutionary path of the system's greenwashing density.

To provide a quantitative comparison of the three initial hub strategy configurations, Table 4 summarizes their terminal greenwashing densities, 95% confidence intervals, quasi-convergence indicators, and homogeneous absorption outcomes.

The results indicate that Scenario B produces the highest terminal greenwashing density, followed by Scenario C and Scenario A. The absorption rates are 90%, 95%, and 65%, respectively. Scenario C also exhibits the lowest absorption frequency and the largest mean observed quasi-convergence step, indicating more persistent variation in the evolutionary trajectories within the observation horizon.

**Table 4.** Terminal outcomes under three hub initial strategies.

| Indicator | Scenario A | Scenario B | Scenario C |
|---|---|---|---|
| Mean terminal greenwashing density | 0.4320 | 0.9675 | 0.7195 |
| 95%confidence interval | [0.2014, 0.6626] | [0.8995, 1.0000] | [0.5251, 0.9139] |
| Quasi-convergence rate | 90.0% | 100.0% | 85.0% |
| Mean quasi-convergence step | 388.00 | 281.35 | 476.12 |
| Absorption rate | 90.0% | 95.0% | 65.0% |
| Mean absorption time among absorbed runs | 412.89 | 323.74 | 502.46 |

To evaluate the statistical differences among scenarios, a Friedman test is performed using the 20 matched replicates. The test identifies a significant overall difference ($\chi_F^2 = 13.614$, $p = 0.00111$). Subsequent paired Wilcoxon signed-rank tests with Holm correction indicate significant differences between Scenarios A and B ($p_{\text{adj}} = 0.00240$) and between Scenarios B and C ($p_{\text{adj}} = 0.03168$). However, the difference between Scenarios A and C is not statistically significant ($p_{\text{adj}} = 0.08481$).

The corresponding mean terminal density differences are −0.5355 for A versus B, −0.2875 for A versus C, and 0.2480 for B versus C. These findings provide statistical evidence that the all-greenwashing hub configuration generates higher terminal greenwashing density than the other two configurations under the fixed network design. Nevertheless, the nonsignificant A–C comparison does not establish equivalence between these scenarios.

Importantly, the scenarios differ in their initial numbers of greenwashing hub firms, and therefore also in the total initial greenwashing count. Consequently, this experiment assesses the combined consequences of alternative initial strategy configurations of the hubs rather than isolating a pure network position effect. The latter issue is investigated separately in Experiment 5 through controls that hold the total number of initially greenwashing firms constant.

### 5.2.3. Visual display of network snapshots

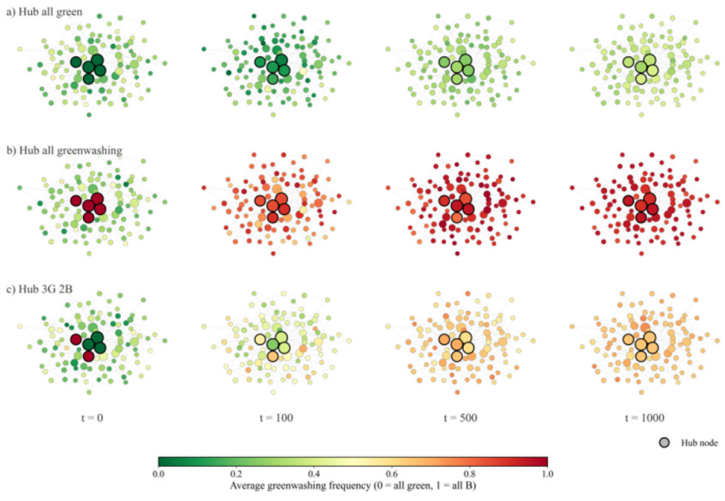



**Figure 3.** Evolution of network strategy snapshots under three initial hub strategy scenarios.

Figure 3 shows the average greenwashing frequency of each node across the 20 replicates, at four time points $t$ = 0, 100, 500, 1000, under the three scenarios.

### *5.3. Experiment 2: Effect of the fuzzy payoff interval width on strategy evolution*

#### 5.3.1. Experimental setup

This experiment, under the initial hub strategy setting of "two greenwashing and three true green", explores the impact of varying degrees of market uncertainty—when all four game payoff parameters are subject to different levels of fuzziness—on the system's convergence rate and final state. Three fuzziness levels are set: Low fuzziness, medium fuzziness, and high fuzziness, by proportionally scaling the interval widths of the triangular fuzzy numbers. The complete triangular fuzzy payoff specifications for the low-, medium-, and high-uncertainty conditions are presented in Table 5.

The triangular fuzzy parameters represent the pessimistic, realistic (most likely), and optimistic values, respectively. The interval width is defined as $D_X = X^o - X^p$.

**Table 5**. Payoff interval parameter settings under different fuzziness levels.

| Fuzziness level | *R* | *S* | *T* | *P* |
|---|---|---|---|---|
| Low | (0.11, 0.12, 0.13) | (−0.025, −0.02, −0.015) | (0.18, 0.20, 0.22) | (−0.035, −0.03, −0.025) |
| Medium | (0.08, 0.12, 0.16) | (−0.04, −0.02, 0.00) | (0.14, 0.20, 0.26) | (−0.06, −0.03, 0.00) |
| High | (0.02, 0.12, 0.22) | (−0.08, −0.02, 0.04) | (0.06, 0.20, 0.34) | (−0.09, −0.03, 0.03) |

Because the three fuzziness levels are symmetric, the weighted defuzzification operator ($X^p$ + $2X^r$ + $X^o$) / 4 and the expected value of the triangular probability distribution ($X^p$ + $X^r$ + $X^o$) / 3 yield the same central payoff. Therefore, the homogeneous mean-field reference equilibrium is identical across the three levels

$$f^* = \frac{T-R}{(T-R)+(S-P)} = \frac{0.20-0.12}{0.08+0.01} \approx 0.8889 \tag{33}$$

This value is the interior equilibrium of the homogeneous replicator dynamics, not the exact phase transition threshold of the BA network. By keeping the central payoff levels fixed, this experiment isolates the effect of payoff fluctuation magnitude on the evolutionary outcome.

To reduce the dependence of the results on a single network realization, the revised experiment considers 20 independently generated BA networks. For each network and experimental condition, 20 Monte Carlo replicates are conducted over 1000 time steps, resulting in 400 simulation runs per condition. The initial strategy configurations are matched across experimental conditions within each network replicate. Statistical comparisons and confidence intervals are based on the 20 network-level means rather than treating all simulation runs as independent observations.

#### 5.3.2. Evolutionary curve comparison analysis

Figure 4 shows the mean evolutionary trajectories of the greenwashing density under the three fuzziness levels, together with the 95% confidence bands across 20 replicates.

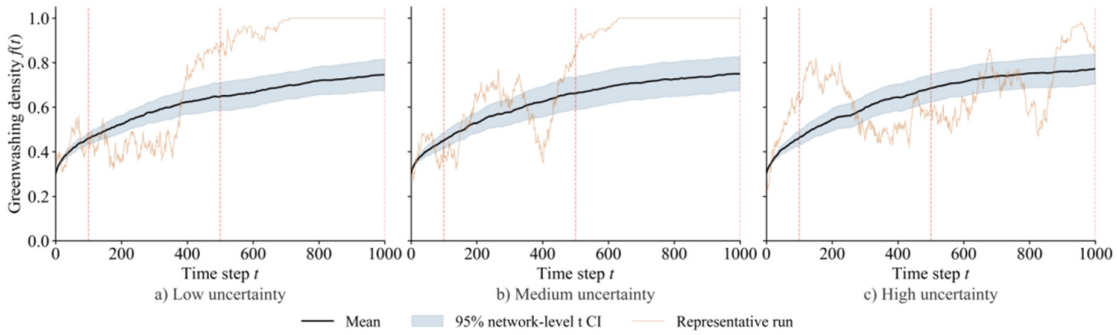



**Figure 4.** Evolution of global greenwashing density under different fuzziness levels.

All three trajectories rise over time and stabilize at high levels, but the confidence bands overlap substantially throughout the evolution. This suggests that the degree of payoff uncertainty has limited influence on the average evolutionary path.

Under all three uncertainty levels, the average greenwashing density increases over time. The trajectories remain relatively close, with substantially overlapping confidence bands. The mean terminal densities are 0.7449, 0.7497, and 0.7731 for low, medium, and high uncertainty, respectively. Although the high-uncertainty condition produces a slightly higher terminal mean, the differences are modest compared with the variability across network realizations.

**Table 6.** Terminal outcomes under different fuzziness levels and the deterministic benchmark.

| Condition | Mean $f(1000)$ | 95%CI | Absorption rate |
|---|---|---|---|
| Low uncertainty | 0.7449 | [0.6743, 0.8155] | 79.0% |
| Medium uncertainty | 0.7497 | [0.6730, 0.8264] | 77.0% |
| High uncertainty | 0.7731 | [0.7060, 0.8402] | 78.5% |
| Deterministic benchmark | 0.7522 | [0.6746, 0.8299] | 81.0% |

Table 6 summarizes the terminal outcomes under the three uncertainty levels and the deterministic benchmark. The deterministic condition yields a mean terminal greenwashing density of 0.7522, comparable with those obtained under stochastic payoff sampling. A Friedman test based on the 20 matched network-level means does not identify a statistically significant difference among the four conditions ($\chi^2 = 2.1600, p = 0.5399$). All pairwise Wilcoxon signed-rank comparisons are also nonsignificant after Holm adjustment.

These findings indicate that within the tested parameter ranges, increasing symmetric payoff interval widths does not produce a statistically detectable change in the terminal greenwashing density. However, statistical nonsignificance does not establish equivalence or the absence of uncertainty effects under other payoff configurations.

### 5.3.3. Visual display of network snapshots

Figure 5 presents the spatial evolution states of the network at four time points ($t = 0$, 100, 500, 1000) under different fuzziness levels.

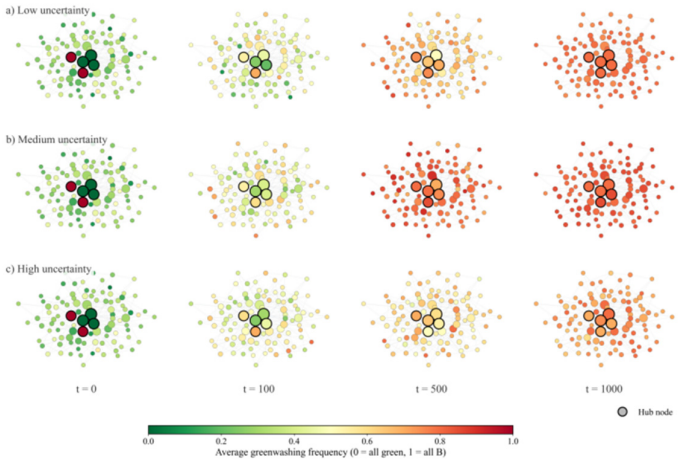



**Figure 5**. Comparison of the evolution of network strategy snapshots under different fuzziness levels.

As time progresses, the greenwashing frequency of nodes gradually increases, but noticeable spatial heterogeneity remains among the different fuzziness levels. This indicates that the magnitude of payoff fluctuations and local network interactions jointly affect the node-level strategy distribution. It should be noted that the intermediate colors in the map of average frequency only represent the frequency of the strategies' occurrence across replicates and do not imply that firms adopt a third mixed strategy.

### 5.3.4. Defuzzification operator sensitivity

To further examine whether the choice of defuzzification operator affects the conclusions, an auxiliary asymmetric payoff configuration is used in which the two operators $(X^p + 2X^r + X^o) / 4$ and $(X^p + X^r + X^o) / 3$ no longer yield identical expected values. Table 7 compares the weighted and centroid defuzzification operators under the asymmetric payoff configuration, reporting their corresponding homogeneous mean-field reference equilibria, mean terminal greenwashing densities, and 95% confidence intervals.

**Table 7.** Comparison of defuzzification operators under an asymmetric payoff configuration.

| Operator | $f^*$ | $f(1000)$ | 95% CI |
|---|---|---|---|
| Weighted $(X^p + 2X^r + X^o) / 4$ | 0.8919 | 0.7722 | [0.7095, 0.8349] |
| Centroid $(X^p + X^r + X^o) / 3$ | 0.8929 | 0.7442 | [0.6767,0.8116] |

The two operators yield closely positioned mean-field reference equilibria (0.8918 and 0.8929), while the corresponding mean terminal greenwashing densities are 0.7722 and 0.7442. A paired Wilcoxon signed-rank test based on network-level means does not identify a statistically significant difference ($p = 0.2774$). Therefore, the present results do not provide sufficient evidence of a systematic difference between the two operators under this asymmetric payoff configuration.

For the assumed triangular probability distribution, the probabilistic expectation coincides numerically with the centroid operator. This does not imply equivalence with every possible definition

of fuzzy expectation. Accordingly, the present analysis is restricted to the specified weighted and centroid operators, and no general equivalence is claimed.

#### 5.3.5. Robustness to stochastic payoff-sampling mechanisms

To assess whether the evolutionary outcomes depend on the stochastic payoff realization mechanism, three alternative specifications are compared: Comparison-level resampling, edge-fixed sampling, and run-fixed sampling. The first independently redraws bilateral payoffs during each local payoff evaluation; the second fixes payoff realizations for each directed edge and strategy combination within a simulation run; and the third draws one payoff vector $(R, S, T, P)$ at the beginning of each run and maintains it throughout its evolution.

Under the three mechanisms, the mean terminal greenwashing densities are 0.7480, 0.7167, and 0.6664, respectively, with network-level 95% confidence intervals of [0.6738, 0.8221], [0.6220, 0.8114], and [0.6150, 0.7177]. A Friedman test based on 20 matched network-level means identifies an overall difference among the three mechanisms ($\chi^2 = 6.1000$, $p = 0.0474$. Subsequent paired Wilcoxon signed-rank tests with Holm correction indicate a statistically significant difference between comparison-level and run-fixed sampling ($p_{\text{adj}} = 0.0459$), while the remaining pairwise differences are not statistically significant.

These findings suggest that the temporal persistence of stochastic payoff realizations can influence the evolution of greenwashing under the investigated conditions. In particular, comparison-level resampling produces a higher mean terminal greenwashing density than run-fixed sampling. Nevertheless, the results should not be interpreted as establishing the superiority of a particular sampling mechanism, since each specification represents a different assumption about the realization of uncertain interaction payoffs.

### *5.4. Experiment 3: Extreme boundary values and mean-controlled comparison*

#### 5.4.1. Experimental setup

This experiment examines how extreme boundary values of the fuzzy payoffs affect the evolutionary outcome. Two subexperiments are conducted.

Experiment 3A: Extreme boundary adjustment. Three scenarios are constructed, as shown in Table 8. Scenario A is the baseline. In Scenario B, the optimistic value of the speculative payoff of greenwashing $T^o$ is raised from 0.26 to 0.45, simulating a period of loose regulation with a wide speculative window. In Scenario C, the pessimistic value of the payoff of genuine green strategies $R^p$ is lowered from 0.08 to 0.01, simulating a situation in which genuine green strategies lack a minimum payoff guarantee. The parameters $S$ and $P$ remain unchanged across all scenarios.

**Table 8.** Fuzzy payoff parameters in Experiment 3A.

| Scenario | *R* | *S* | *T* | *P* |
|---|---|---|---|---|
| A: Baseline | (0.08, 0.12, 0.16) | (−0.04, −0.02, 0.00) | (0.14, 0.20, 0.26) | (−0.06, −0.03, 0.00) |
| B: High $T^o$ | (0.08, 0.12, 0.16) | (−0.04, −0.02, 0.00) | (0.14, 0.20, 0.45) | (−0.06, −0.03, 0.00) |
| C: Low $R^p$ | (0.01, 0.12, 0.16) | (−0.04, −0.02, 0.00) | (0.14, 0.20, 0.26) | (−0.06, −0.03, 0.00) |

The triangular fuzzy parameters represent the pessimistic, realistic, and optimistic values. In Scenario B, the optimistic value of $T$ is raised; in Scenario C, the pessimistic value of $R$ is lowered.

It should be noted that adjusting the extreme boundary values in Scenarios B and C also changes the corresponding expected defuzzified values. Using the weighted operator $E_w(\tilde{X}) = (X^p + 2X^r + X^o) / 4$, the expected defuzzified values and the homogeneous mean-field reference thresholds are reported in Table 9.

**Table 9.** Defuzzified payoffs and mean-field reference equilibria in Experiment 3A.

| Scenario | $E_w(R)$ | $E_w(S)$ | $E_w(T)$ | $E_w(P)$ | $f^*$ |
|---|---|---|---|---|---|
| A: Baseline | 0.1200 | −0.0200 | 0.2000 | −0.0300 | 0.8889 |
| B: High $T^o$ | 0.1200 | −0.0200 | 0.2475 | −0.0300 | 0.9273 |
| C: Low $R^p$ | 0.1025 | −0.0200 | 0.2000 | −0.0300 | 0.9070 |

Thus, the differences observed in Experiment 3A reflect the joint effect of boundary shifts and changes in expected value.

Experiment 3B: Mean-controlled design. To isolate the effect of interval width, three scenarios (L, M, H) are constructed with identical expected defuzzified values $E_w(R) = 0.12$, $E_w(S) = -0.02$, $E_w(T) = 0.20$ and $E_w(P) = -0.03$, but different interval widths. The parameters are shown in Table 10.

**Table 10.** Fuzzy payoff parameters in Experiment 3B.

| Scenario | $R$ | $T$ | $D_R$ | $D_T$ |
|---|---|---|---|---|
| L: Low width | (0.10, 0.12, 0.14) | (0.18, 0.20, 0.22) | 0.04 | 0.04 |
| M: Medium width | (0.08, 0.12, 0.16) | (0.14, 0.20, 0.26) | 0.08 | 0.12 |
| H: High width | (0.04, 0.12, 0.20) | (0.10, 0.20, 0.30) | 0.16 | 0.20 |

Both subexperiments are conducted on 20 independently generated BA networks, with 20 Monte Carlo replicates per network and 1000 time steps per replicate. The same network realizations and matched initial strategy configurations are used across conditions within each subexperiment. Statistical inference is based on network-level mean outcomes to avoid treating simulation replicates on the same network as independent observations.

Experiment 3A examines extreme payoff bound adjustments that change both the payoff dispersion and payoff incentives. Experiment 3B complements this analysis by varying the widths of the $R$ and $T$ payoff intervals while keeping their weighted defuzzified values unchanged.

### 5.4.2. Evolutionary curve comparison analysis

Figure 6 shows the mean evolutionary trajectories of the greenwashing density under the three scenarios of Experiment 3A, together with the 95% confidence bands across 20 replicates.

Under Scenario A, the greenwashing density increases gradually and reaches a lower terminal level than those observed under Scenarios B and C.

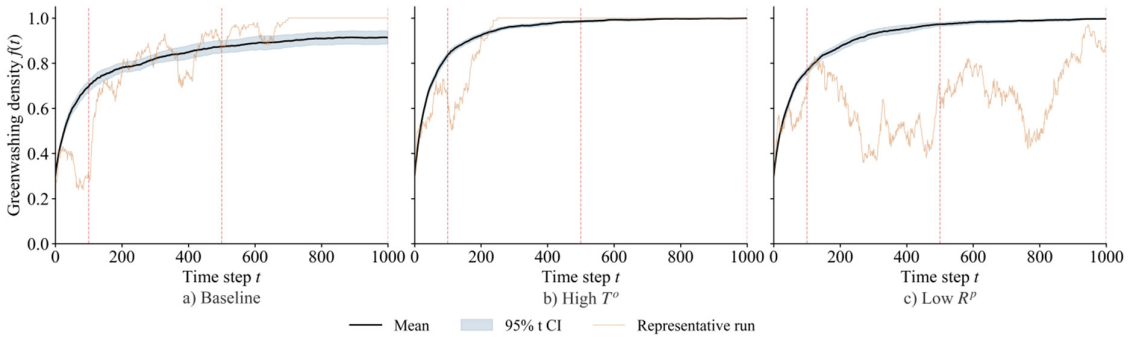



**Figure 6.** Evolutionary trajectories of greenwashing density under extreme boundary scenarios.

Under Scenario A, the mean greenwashing density increases gradually and reaches 0.9138 at $T = 1000$. Under Scenario B, increasing the optimistic bound of the temptation payoff from 0.26 to 0.45 accelerates the diffusion of greenwashing, with the mean terminal density reaching 0.9994. Under Scenario C, reducing the pessimistic bound of the genuine green payoff from 0.08 to 0.01 produces a similar pattern, with a terminal density of 0.9970. Both adjusted scenarios approach the all-greenwashing absorbing state within the simulation horizon.

**Table 11.** Terminal outcomes under extreme boundary scenarios (Experiment 3A).

| Scenario | Mean $f(1000)$ | 95%CI | All green | All B | Mixed |
|---|---|---|---|---|---|
| A: Baseline | 0.9138 | [0.8842, 0.9433] | 17 | 339 | 44 |
| B: High $T^o$ | 0.9994 | [0.9984, 1.0000] | 0 | 396 | 4 |
| C: Low $R^p$ | 0.9970 | [0.9943, 0.9996]. | 0 | 388 | 12 |

Table 11 reports the terminal greenwashing density $f(1000)$, the 95% confidence interval, the decomposition of the absorbing state, and the mean convergence step for each scenario. To determine which extreme payoff bound adjustments are associated with statistically detectable differences in terminal greenwashing density, Table 12 reports the pairwise mean differences and Holm-adjusted $p$-values for the three scenarios.

**Table 12.** Pairwise comparison in Experiment 3A.

| Comparison | Mean difference | Holm-adjusted $p$ |
|---|---|---|
| A vs B | −0.0856 | $5.72 \times 10^{-6}$ |
| A vs C | −0.0832 | $5.72 \times 10^{-6}$ |
| B vs C | 0.0024 | 0.0841 |

A Friedman test based on the 20 matched network-level means identifies a statistically significant overall difference among the three scenarios ($\chi^2 = 34.3333$, $p = 3.50 \times 10^{-8}$). Subsequent paired Wilcoxon signed-rank tests with Holm correction reveal significant differences between Scenarios A and B and between Scenarios A and C (both adjusted $p = 5.72 \times 10^{-6}$). However, the difference between Scenarios Band C is not statistically significant (adjusted $p = 0.0841$).

These results indicate that increasing speculative greenwashing returns or reducing genuine green cooperation payoffs is associated with higher terminal greenwashing density. However, these adjustments also alter the central payoff values, so their effects cannot be attributed solely to changes in the interval width. The nonsignificant difference between Scenarios B and C does not imply equivalence.

### 5.4.3. Visual display of network snapshots

Figure 7 shows the average greenwashing frequency of each node across 20 replicates, at four time points $t = 0$, 100, 500, 1000, under the three scenarios of Experiment 3A.

Under Scenario A, greenwashing gradually spreads across the network, although some spatial heterogeneity remains at the final observation time. Under Scenario B, a higher optimistic temptation payoff is associated with more rapid diffusion of greenwashing, and nearly all nodes exhibit high greenwashing frequencies by $t = 500$. Scenario C displays a similar pattern, with widespread greenwashing during the later stages.

These patterns are consistent with the terminal outcomes reported in Table 11. However, the snapshots provide a descriptive illustration of the evolutionary process rather than independent statistical evidence of the differences among scenarios.

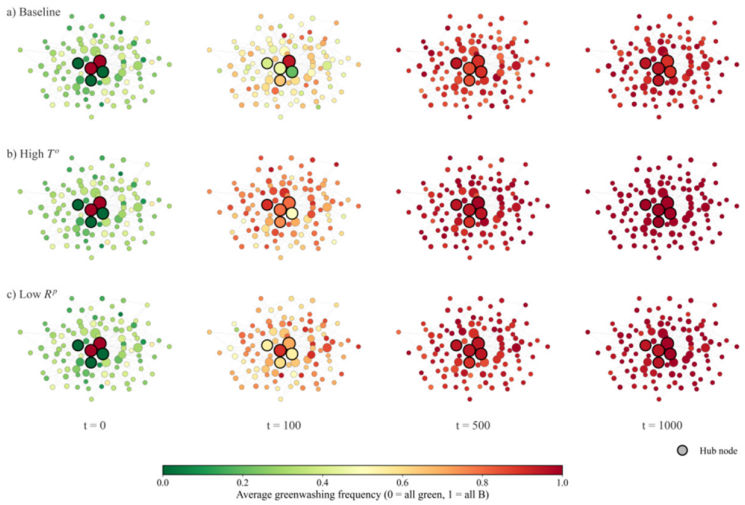



**Figure 7.** Network snapshots of average greenwashing frequency under extreme boundary scenarios.

### 5.4.4. Mean-controlled comparison (Experiment 3B)

Figure 8 illustrates the evolutionary trajectories of greenwashing density under the three mean-controlled payoff interval width configurations. The weighted defuzzified values of the four payoff components remain constant at $R = 0.12$, $S = -0.02$, $T = 0.20$, and $P = -0.03$, while the widths of the $R$ and $T$ payoff intervals are varied.

The three scenarios exhibit similar evolutionary trajectories, with mean greenwashing density increasing throughout the simulation horizon. Although individual simulation runs display noticeable fluctuations, the mean trajectories remain relatively close, and their network-level confidence intervals overlap substantially.

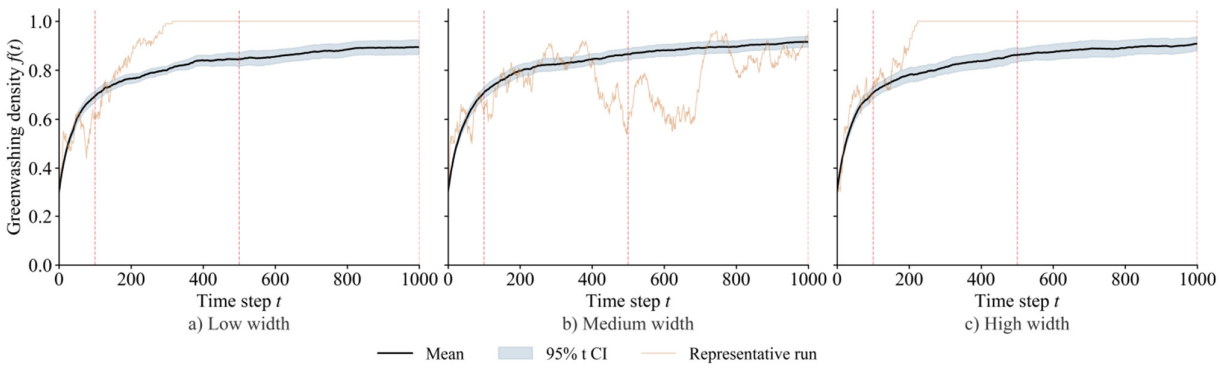



**Figure 8.** Evolutionary trajectories of greenwashing density under different mean-controlled payoff interval widths.

Table 13 reports the terminal outcomes under the three mean-controlled payoff interval width configurations. The mean terminal greenwashing densities are 0.8939, 0.9159, and 0.9084 for low, medium, and high interval widths, respectively.

**Table 13.** Terminal outcomes under mean-controlled interval widths (Experiment 3B).

| Scenario | Mean $f(1000)$ | 95%CI | All green | All B | Mixed |
|---|---|---|---|---|---|
| L: Low width | 0.8939 | [0.8637, 0.9241] | 25 | 325 | 50 |
| M: Medium width | 0.9159 | [0.8945, 0.9372] | 17 | 322 | 61 |
| H: High width | 0.9084 | [0.8797, 0.9370] | 19 | 325 | 56 |

A Friedman test based on 20 matched network-level means does not identify a statistically significant difference among the three conditions ($\chi^2 = 2.8000, p = 0.2466$). Pairwise Wilcoxon signed-rank tests with Holm correction also yield nonsignificant results (L vs. M: $p_{\text{adj}} = 0.3638$; L vs. H: $p_{\text{adj}} = 0.4910$; M vs. H: $p_{\text{adj}} = 0.7012$).

These results indicate that varying the selected payoff interval widths while maintaining identical central payoffs does not produce statistically detectable differences in terminal greenwashing density within the investigated parameter range. Nevertheless, statistical nonsignificance should not be interpreted as evidence that the three configurations are equivalent.

Together with Experiment 3A, this comparison suggests that the strong changes observed under extreme boundary adjustments are associated with changes in payoff incentives as well as uncertainty specifications, rather than demonstrating a general monotonic effect of payoff the interval width alone.

### *5.5. Experiment 4: Interactive effects of social learning intensity and strategic inertia*

#### 5.5.1. Experimental setup

Experiment 4 examines the effects of social learning intensity and strategic inertia on greenwashing's evolution. Three learning intensity levels, $\eta = 0.5$, 1.2, and 2.5, are combined with two

degree-dependent inertia configurations: Low inertia, ($\rho_{min}$, $\rho_{max}$) = (0.2, 0.4), and high inertia, ($\rho_{min}$, $\rho_{max}$) = (0.6, 0.8), yielding six experimental conditions.

The experiment uses 20 independently generated BA networks with $N$ = 100 and $m$ = 3. Each condition is replicated 20 times per network over 1000 evolutionary time steps, resulting in 400 simulations per condition. The initial configuration contains two greenwashing hub firms and three genuinely green hub firms, with 30% of peripheral firms initially adopting greenwashing. Matched initial strategy configurations are used across the six conditions within each network replicate. Statistical comparisons are performed using network-level means.

The triangular payoff parameters follow the baseline configuration in Table 3, and the asynchronous Fermi imitation mechanism remains unchanged. Under the inertia-modified update rule, greater inertia reduces the probability of switching strategy for a given payoff difference, whereas the effect of learning intensity depends on the sign and magnitude of that difference.

### 5.5.2. Evolution of greenwashing density

Figure 9 presents the mean evolutionary trajectories of greenwashing density under the six combinations of learning intensity and strategic inertia. Subplots (a)–(c)correspond to $\eta$ = 0.5, 1.2, and 2.5, respectively. The solid blue curves represent low-inertia conditions, while the dashed red curves represent high-inertia conditions. The shaded bands indicate 95% confidence intervals based on network-level means.

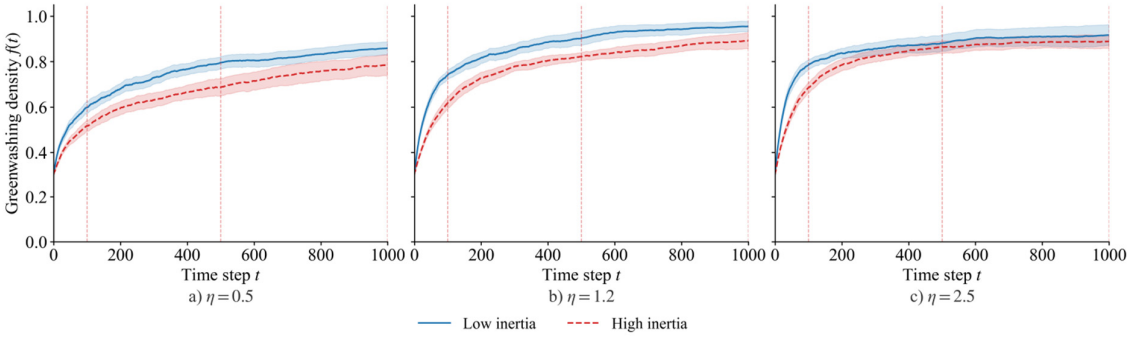



**Figure 9.** Evolutionary trajectories of greenwashing density under different learning intensities and inertia configurations.

### 5.5.3. Terminal outcomes

Table 14 summarizes the terminal greenwashing densities, network-level 95% confidence intervals, and absorbing state outcomes under the six combinations of social learning intensity and strategic inertia.

Under low inertia, the mean terminal greenwashing density increases from 0.8594 at $\eta$ = 0.5 to 0.9545 at $\eta$ = 1.2, before decreasing to 0.9160 at $\eta$ = 2.5. Under high inertia, the corresponding terminal densities are 0.7838, 0.8925, and 0.8887.

At each learning intensity, the high-inertia configuration produces a lower mean terminal greenwashing density than the low-inertia configuration. The differences are 0.0756, 0.0620, and 0.0273 at $\eta$ = 0.5, 1.2, and 2.5, respectively.

**Table 14.** Terminal outcomes under different learning intensities and inertia configurations.

| $\eta$ | Inertia | Mean $f(1000)$ | 95% CI | All green | All B | Not absorbed |
|---|---|---|---|---|---|---|
| 0.5 | Low | 0.8594 | [0.8310, 0.8877] | 48 | 313 | 39 |
| 0.5 | High | 0.7838 | [0.7381, 0.8295] | 27 | 181 | 192 |
| 1.2 | Low | 0.9545 | [0.9318, 0.9772] | 14 | 368 | 18 |
| 1.2 | High | 0.8925 | [0.8576, 0.9274] | 10 | 260 | 130 |
| 2.5 | Low | 0.9160 | [0.8704, 0.9616] | 22 | 347 | 31 |
| 2.5 | High | 0.8887 | [0.8588, 0.9186] | 2 | 273 | 125 |

The absorption outcomes also vary across inertia configurations. High-inertia conditions exhibit lower absorption rates within the 1000-step horizon (52.00%, 67.50%, and 68.75% for $\eta$ = 0.5, 1.2, 2.5, respectively) compared with the low-inertia conditions (90.25%, 95.50%, and 92.25%). This suggests that greater resistance to strategy switching can delay the attainment of homogeneous absorbing states. Nevertheless, terminal density and absorption are distinct outcomes, and these descriptive differences do not independently establish an interaction effect between learning intensity and inertia.

### 5.5.4. Statistical comparison

To evaluate the effects of learning intensity and strategic inertia, statistical comparisons are conducted using the 20 matched network-level means. Learning intensity is examined by comparing terminal densities averaged across the two inertia configurations, while the overall inertia effect is assessed using paired differences averaged across the three learning intensity levels. The statistical comparisons are summarized in Table 15, including the overall effects of learning intensity and strategic inertia and the test of their interaction based on paired network-level contrasts.

**Table 15.** Pairwise comparison between low and high inertia at each learning intensity.

| Effect | Test | Statistic | $p$-value |
|---|---|---|---|
| Learning intensity | Friedman | $x^2 = 17.1000$ | 0.000194 |
| Strategic inertia | Paired Wilcoxon | $W = 7.0$ | 0.0000362 |
| Learning intensity × inertia | Friedman on paired contrasts | $x^2 = 4.3000$ | 0.1165 |

The Friedman test identifies a statistically significant overall difference among learning intensity levels ($\chi^2$ = 17.1000, $p$ = 0.000194). Subsequent paired Wilcoxon signed-rank tests with Holm correction indicate significant differences between $\eta$ = 0.5 and $\eta$ = 1.2 ($p_{\text{adj}}$ = 0.000109) and between $\eta$ = 0.5 and $\eta$ = 2.5 ($p_{\text{adj}}$ = 0.00631). However, the difference between $\eta$ = 1.2 and $\eta$ = 2.5 is not statistically significant ($p_{\text{adj}}$ = 0.2396).

For strategic inertia, the mean difference between low- and high-inertia configurations, averaged across learning intensity levels, is 0.0550, with a 95%confidence interval of [0.0333, 0.0766]. The paired Wilcoxon signed-rank test indicates a statistically significant overall inertia effect ($p$ = 0.0000362). This finding suggests that higher inertia is associated with lower terminal greenwashing density under the investigated configurations.

To formally examine the interaction between learning intensity and strategic inertia, the high minus low inertia contrast is calculated for each learning intensity within every network realization. The mean contrasts are −0.075, −0.0620, and −0.0273 at $\eta$ = 0.5, 1.2, and 2.5, respectively.

Although the magnitude of the inertia contrast decreases numerically as the learning intensity increases, a Friedman test does not identify a statistically significant difference among these contrasts ($\chi^2$ = 4.3000, $p$ = 0.1165). All pairwise comparisons are also nonsignificant after Holm correction. Therefore, the present evidence supports separate effects of learning intensity and strategic inertia but does not establish a statistically significant interaction between them.

These findings should be interpreted within the tested parameter ranges and network configurations rather than as evidence of universally optimal learning intensity or inertia levels.

### 5.5.5. Network snapshots

Figure 10 shows the average greenwashing frequency of each node across the 20 replicates, at four time points $t$ = 0, 100, 500, 1000, under the six conditions.

Rows correspond to low and high inertia; columns correspond to the three learning intensities and four time points. Node colors indicate the average frequency with which a node adopts the greenwashing strategy over 20 replicates. Hub nodes are highlighted with thick black outlines, and a horizontal color bar is placed at the bottom.

Under low inertia, the network at $\eta$ = 1.2 and $\eta$ = 2.5 turns deep red by $t$ = 500, indicating the rapid diffusion of greenwashing across the whole network. Under high inertia, even at $\eta$ =2.5, a noticeable number of orange and yellow-green nodes remain, indicating that inertia delays the complete lock-in of greenwashing. In addition, under high inertia, the hub nodes exhibit greater heterogeneity in their strategy distribution, with some hubs maintaining relatively low greenwashing frequencies across most replicates.

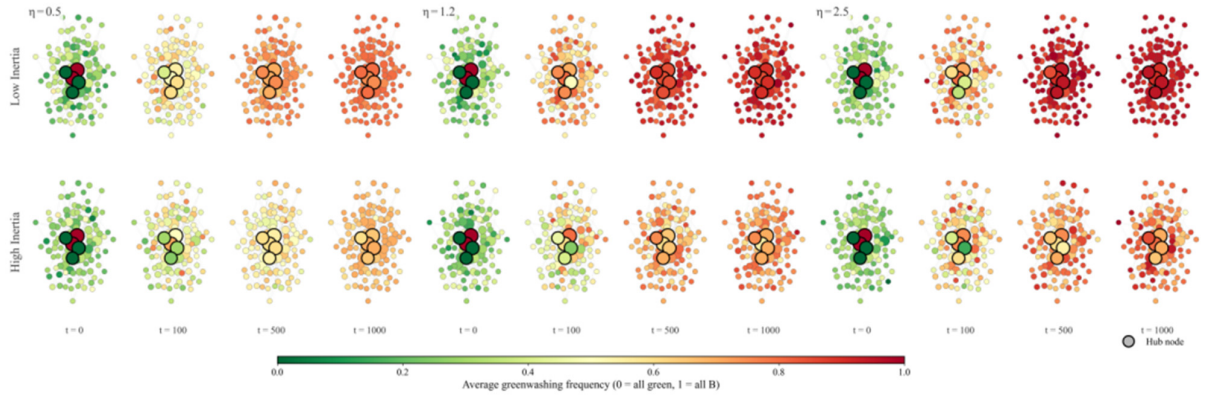



**Figure 10.** Network snapshots of average greenwashing frequency under different learning intensities and inertia configurations.

### *5.6. Experiment 5: Sensitivity analysis of BA network parameters and hub strategy configuration*

#### 5.6.1. Experimental setup

Experiment 5 examines how the network's topology, the initial placement of greenwashing, payoff evaluation, and strategic inertia influence greenwashing's evolution. Five subexperiments are conducted to evaluate the conditional effects of these mechanisms.

Experiment 5A investigates the BA attachment parameter $m$ = 2, 3, 5 under a fixed network size $N$ = 100. Experiment 5B compares three initial placement configurations for greenwashing—high-degree, random, and low-degree—while fixing the total number of initial greenwashing firms at 30. Experiment 5C compares accumulated and degree-normalized payoff evaluation across the three attachment parameters. To ensure consistency, the accumulated payoff results from Experiment 5A are reused directly in Experiment 5C.

Experiment 5D extends the robustness analysis to network sizes $N$ = 100, 200, 300, hub counts $K$= 3, 5, 10, and four inertia specifications: degree-dependent, constant, reverse-degree, and random inertia. Experiment 5E further examines the conditional effects of the initial placement of greenwashing by comparing the baseline model, degree-normalized payoffs, the removal of strategic inertia, and the combination of both modifications.

Each experimental condition is evaluated using 20 independent BA network realizations, with 20 Monte Carlo replicates per network and 1000 evolutionary time steps per replicate. Statistical inference is based on network-level means. Friedman tests are used for overall comparisons, followed by paired Wilcoxon signed-rank tests with Holm adjustment where appropriate. The baseline triangular payoff specifications, stochastic payoff sampling assumption, and asynchronous Fermi imitation rule remain consistent with Section 5.1.

#### 5.6.2. Subexperiment 5A: Effect of the BA connection parameter on the terminal state

Experiment 5A examines the sensitivity of terminal greenwashing density to the BA attachment parameter $m$. Table 16 presents the terminal outcomes under the three network configurations.

**Table 16.** Terminal outcomes under different BA attachment parameters.

| Configuration | Mean $f(1000)$ | 95% CI | Absorption rate |
|---|---|---|---|
| $m = 2$ | 0.6531 | [0.5526, 0.7536] | 79.0% |
| $m = 3$ | 0.8776 | [0.8140, 0.9411] | 80.5% |
| $m = 5$ | 0.9973 | [0.9940, 1.0000] | 98.0% |

The mean terminal greenwashing density increases from 0.6531 at $m$ = 2 to 0.8776 at $m$ = 3, reaching 0.9973 at $m$ = 5. The corresponding absorption rates are 79.0%, 80.5%, and 98.0%, respectively, indicating that the configuration with the highest connectivity is more frequently absorbed within the simulation horizon.

A Friedman test based on the 20 matched network-level means identifies a significant overall difference among the three attachment parameters ($\chi^2$ = 18.2000, $p$ = 0.000112). Subsequent paired Wilcoxon signed-rank tests with Holm adjustment indicate significant differences among all three pairs (all adjusted $p$ = 0.00586).

These findings indicate that greater BA connectivity is associated with higher terminal greenwashing density under the accumulated payoff specification. However, increasing $m$ changes both the network connectivity and the number of bilateral interactions contributing to accumulated payoffs. Therefore, the observed differences cannot be attributed exclusively to the network's structure. The contribution of payoff accumulation is examined separately in Experiment 5C.

### 5.6.3. Evolutionary curve comparison

Figure 11 illustrates the mean evolutionary trajectories of greenwashing density under the three BA attachment parameters. The solid curves represent the average trajectories across network realizations, and the shaded regions indicate 95% confidence intervals based on network-level means.

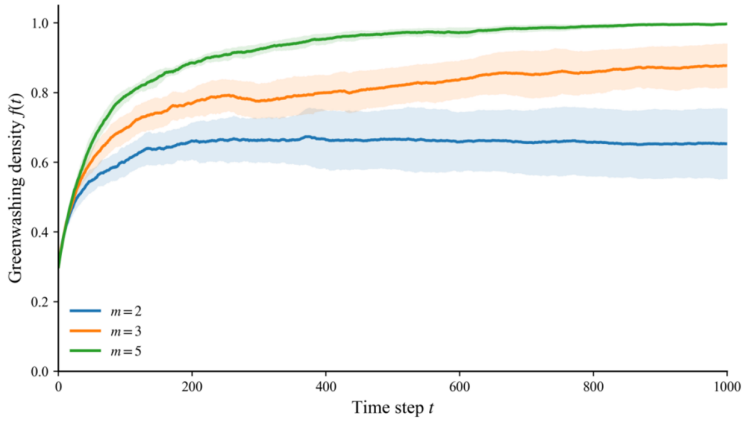



**Figure 11**. Evolutionary trajectories of greenwashing density under different BA attachment parameters.

All three configurations exhibit increasing greenwashing density during the evolutionary process. However, the trajectories diverge as evolution proceeds. Under $m = 2$, the mean density increases initially but subsequently remains around 0.65 during the later stages. Under $m = 3$, greenwashing continues to spread and approaches 0.88 at the final observation time. Under $m = 5$, the mean density increases more rapidly and approaches the all-greenwashing absorbing state.

### 5.6.4. Sub-experiment 5B: Effect of greenwashing's initial placement

Experiment 5B investigates whether greenwashing's initial placement affects the evolutionary outcomes when the total number of initially greenwashing firms is fixed at 30. Three configurations are compared: Placement among the 30 highest-degree nodes, random placement, and placement among the 30 lowest-degree nodes. Table 17 presents the terminal greenwashing densities and associated uncertainty estimates for the high-degree, random, and low-degree placement configurations, with the total number of initial greenwashing enterprises fixed at 30.

The high-degree placement produces the highest mean terminal greenwashing density (0.9609), followed by random placement (0.7744) and low-degree placement (0.3609). The difference between

the high- and low-degree configurations reaches approximately 0.6000, indicating substantial sensitivity to the initial network position.

**Table 17.** Terminal outcomes under different initial greenwashing placements.

| Initial placement | Mean $f(1000)$ | 95% CI | Absorption rate |
|---|---|---|---|
| High-degree | 0.9609 | [0.9348, 0.9869] | 93.0% |
| Random | 0.7744 | [0.6742, 0.8745] | 75.5% |
| Low-degree | 0.3609 | [0.2086, 0.5132] | 90.5% |

A Friedman test identifies a significant overall difference among the three placement configurations ($\chi^2 = 20.0000$, $p = 4.54 \times 10^{-5}$). All three paired comparisons remain significant after Holm adjustment (adjusted$p = 0.00586$).

These results suggest that the initial placement of greenwashing among highly connected firms is associated with substantially greater subsequent diffusion under the baseline model. Because the initial number of greenwashing firms and the network configurations are controlled, the differences cannot be explained solely by the initial prevalence of greenwashing.

However, highly connected nodes also accumulate more bilateral payoffs and are assigned different inertia values under the baseline model. Therefore, the results do not independently identify a pure network position effect. Experiments 5C and 5E further examine the contribution of these mechanisms.

### 5.6.5. Subexperiment 5C: Role of the payoff accumulation mechanism

Experiment 5C compares accumulated and degree-normalized payoffs under the three BA attachment parameters. The accumulated payoff results are identical to those reported in Experiment 5A, ensuring consistency between the two subexperiments. Table 18 compares the terminal greenwashing outcomes under accumulated and degree-normalized payoff evaluation for the three BA attachment parameters ($m$ = 2, 3, and 5). The accumulated payoff entries are taken from Experiment 5A to ensure consistency between the two subexperiments.

**Table 18.** Terminal outcomes under accumulated and degree-normalized payoffs.

| Configuration | Accumulated payoff | Degree-normalized payoff | Mean difference |
|---|---|---|---|
| $m = 2$ | 0.6531 | 0.5814 | 0.0717 |
| $m = 3$ | 0.8776 | 0.6188 | 0.2588 |
| $m = 5$ | 0.9973 | 0.6298 | 0.3675 |

Under accumulated payoffs, the terminal greenwashing density increases substantially as $m$ increases. In contrast, the corresponding densities under degree-normalized payoffs are 0.5814, 0.6188, and 0.6298, showing much smaller numerical variation across network configurations.

A Friedman test across the six configurations identifies an overall difference ($\chi^2 = 33.0286$, $p = 3.71 \times 10^{-6}$). However, when all 15 pairwise comparisons are adjusted using the Holm procedure, the accumulated versus normalized comparison is significant at $m = 5$ (adjusted $p = 0.0293$), but not at $m = 2$ (adjusted $p = 1.0000$) or $m = 3$ (adjusted $p = 0.0684$).

These results indicate that the accumulation of payoff contributes to the observed sensitivity to BA connectivity. Degree normalization substantially reduces the numerical differences across network configurations, particularly at higher connectivity levels. Nevertheless, degree normalization does not eliminate the effects of network topology on neighbor selection or social imitation, and the present results do not establish complete independence from the network's structure.

#### 5.6.6. Robustness to network size, hub classification, and strategic inertia (Experiment 5D)

Experiment 5D extends the sensitivity analysis by varying the network size, hub count, and the relationship between network degree and strategic inertia.

For network size, the mean terminal greenwashing densities are 0.8752, 0.8198, and 0.7219 at $N$ = 100, 200, and 300, respectively. The Friedman test identifies an overall difference ($p$ = 0.000371). Holm-adjusted pairwise tests indicate significant differences between $N$ = 100 and $N$ = 300 and between $N$ = 200 and $N$ =300 (both adjusted $p$ = 0.00586), whereas the difference between $N$ = 100 and $N$ =200 is not significant (adjusted $p$ = 0.0645).

The absorption rates also decrease from 86.0% at $N$ =100 to 57.5% at $N$ = 200 and 31.5% at $N$ = 300. Therefore, the lower terminal densities in larger networks should be interpreted within the fixed 1000-step horizon rather than as evidence that increasing the network size necessarily suppresses greenwashing in the long run.

When the hub count is varied across $K$ = 3, 5, 10, the corresponding terminal densities are 0.9449, 0.9324, and 0.8982. The Friedman test does not identify a significant overall difference ($p$ = 0.2725). Because changing the hub count also affects the initialization of hub strategies, these outcomes represent sensitivity to the hub configuration rather than a pure classification effect.

Finally, degree-dependent, constant, reverse-degree, and random inertia yield mean terminal densities of 0.9274, 0.9422, 0.9412, and 0.9724, respectively. The overall Friedman test is not statistically significant ($p$ = 0.0560), and none of the pairwise comparisons remains significant after Holm correction.

Taken together, Experiment 5D indicates that finite-horizon outcomes are sensitive to network size, whereas the selected hub count and inertia specifications do not produce statistically detectable overall differences within the present design. These results also demonstrate that the findings should not be generalized independently of the network size, observation horizon, or initialization procedures.

#### 5.6.7. Mechanism ablation of greenwashing's initial placement (Experiment 5E)

Experiment 5E further examines the relationship between the initial placement of greenwashing, payoff accumulation, and strategic inertia. The total number of initial greenwashing firms remains fixed at 30, and three placement configurations are examined under four behavioral mechanisms.

The baseline mechanism combines accumulated payoffs with degree-dependent inertia. The alternative specifications use degree-normalized payoffs, removal of strategic inertia, or both modifications simultaneously. Table 19 summarizes the terminal greenwashing densities under 12 experimental configurations combining three initial strategy placement patterns with four payoff evaluation and inertia mechanisms. These comparisons help assess the sensitivity of placement effects to alternative behavioral assumptions.

**Table 19.** Terminal greenwashing densities under alternative placement and behavioral mechanisms.

| Initial placement | Baseline | No inertia | Normalized | Both |
|---|---|---|---|---|
| High-degree | 0.9609 | 0.9655 | 0.8638 | 0.8099 |
| Random | 0.7744 | 0.9322 | 0.5398 | 0.6115 |
| Low-degree | 0.3609 | 0.4600 | 0.2901 | 0.4424 |

Under the baseline mechanism, high-degree placement produces the highest terminal greenwashing density, followed by random and low-degree placements. This ordering is also observed descriptively under the three alternative behavioral mechanisms.

Degree normalization reduces the mean terminal greenwashing density for all three placement configurations. For example, under high-degree placement, the mean decreases from 0.9609 to 0.8638, while under random placement, it decreases from 0.7744 to 0.5398. However, removing strategic inertia alone does not consistently reduce greenwashing. Under random placement, the terminal density increases from 0.7744 to 0.9322, while under low-degree placement, it increases from 0.3609 to 0.4600.

The high minus low placement difference decreases from approximately 0.6000 under the baseline mechanism to 0.5737 with degree-normalized payoffs and 0.3675 when normalization and inertia removal are combined. These numerical changes indicate that the magnitude of the placement effect depends on the payoff and behavioral specifications.

A Friedman test across all 12 conditions identifies an overall difference ($\chi^2 = 94.7042$, $p < 0.001$). However, none of the 66 pairwise comparisons remains statistically significant after Holm correction across the full comparison family. Therefore, the numerical differences are interpreted primarily as descriptive evidence of conditional mechanisms rather than as statistically established effects for every individual contrast. To illustrate how the different behavioral mechanisms influence the evolutionary process beyond terminal outcomes, Figure 12 presents the trajectories of greenwashing density under the alternative initial placement and mechanism ablation configurations.

Overall, Experiment 5E suggests that the association between the initial network position and terminal greenwashing remains descriptively evident under several alternative mechanisms, while its magnitude changes with payoff normalization and inertia assumptions. The findings qualify the influence of hub position and do not establish a universally independent hub anchoring effect.

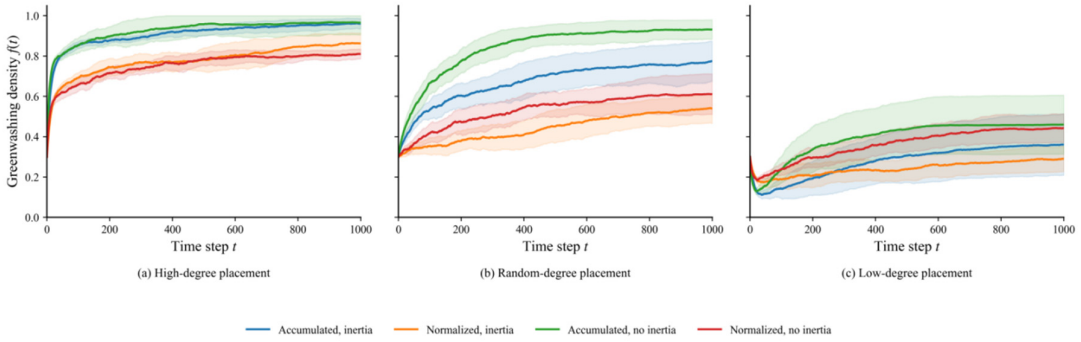



**Figure 12.** Evolutionary trajectories under different initial placements of greenwashing and behavioral mechanisms.

### *5.7. Experiment 6: Robustness check on the initial greenwashing ratio*

#### 5.7.1. Experimental setup

To test whether the baseline conclusions depend on the initial greenwashing ratio of peripheral firms, this experiment varies the initial ratio to 10%, 30%, 50%, and 70%, while keeping the BA network's topology, fuzzy payoff parameters, social learning intensity, strategic inertia, and update mechanism unchanged.

The experiment is conducted on 20 independently generated BA networks with $N = 100$ and $m = 3$. For each network and initial greenwashing condition, 20 Monte Carlo replicates are performed over 1000 time steps, yielding 400 simulation runs per condition. The five hub firms with the highest degree retain the same initial configuration of two greenwashing firms and three genuinely green firms. Nested peripheral greenwashing sets are used across the four conditions within each matched replicate. Statistical inference is based on the 20 independent network-level means.

#### 5.7.2. Evolution of greenwashing density

Figure 13 presents the evolutionary trajectories of greenwashing density under the four initial peripheral greenwashing ratios. The conditions begin with different greenwashing densities, reflecting their initial strategy configurations. The mean terminal greenwashing densities are 0.9373, 0.9315, 0.9474, and 0.9680 for the 10%, 30%, 50%, and 70% conditions, respectively.

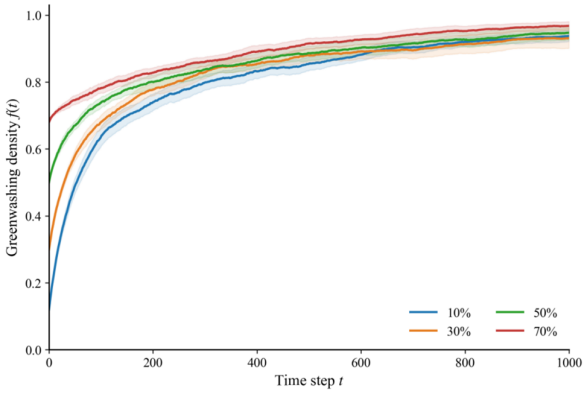



**Figure 13.** Evolutionary trajectories of greenwashing density under different initial ratios.

Despite differences in the initial prevalence of greenwashing, all four conditions exhibit high mean terminal densities. However, the terminal outcomes are not strictly monotonic with respect to the initial ratio. The statistical significance of these differences is examined using matched network-level comparisons in Section 5.7.3.

#### 5.7.3. Terminal outcomes and statistical tests

Table 20 summarizes the terminal greenwashing densities and absorbing state outcomes under the four initial greenwashing ratios.

**Table 20.** Terminal outcomes under different initial greenwashing ratios.

| Initial ratio | Mean $f(1000)$ | 95% CI | All green | All B | Not absorbed |
|---|---|---|---|---|---|
| 10% | 0.9373 | [0.9209, 0.9536] | 12 | 336 | 52 |
| 30% | 0.9315 | [0.9012, 0.9618] | 9 | 326 | 65 |
| 50% | 0.9474 | [0.9262, 0.9685] | 10 | 344 | 46 |
| 70% | 0.9680 | [0.9558, 0.9806] | 4 | 362 | 34 |

The mean terminal densities range from 0.9315 to 0.9680, indicating that greenwashing-dominant outcomes remain prevalent across the tested initial configurations.

A Friedman test based on 20 matched network-level means identifies a statistically significant overall difference among the four conditions ($\chi^2 = 10.2600$, $p = 0.01648$). However, subsequent paired Wilcoxon signed-rank tests with Holm correction do not identify any statistically significant pairwise differences. The smallest adjusted $p$ -value is 0.0566 for the comparison between the 30% and 70% conditions.

The all-greenwashing absorbing state is reached in 336, 326, 344, and 362 out of 400 runs for the four initial ratios, respectively. The corresponding absorption rates, including both homogeneous absorbing states, are 87.0%, 83.75%, 88.5%, and 91.5%. Runs that do not reach an absorbing state within 1000 steps are treated as right-censored in absorption time analysis.

These results suggest that high terminal greenwashing densities occur across a broad range of initial strategy proportions under the tested parameter configuration. Although the overall statistical test detects differences, the pairwise evidence is insufficient to establish which specific initial ratios differ after multiple comparison adjustment. The findings therefore support a conditional robustness interpretation rather than independence from initial conditions.

### 5.7.4. Network snapshots

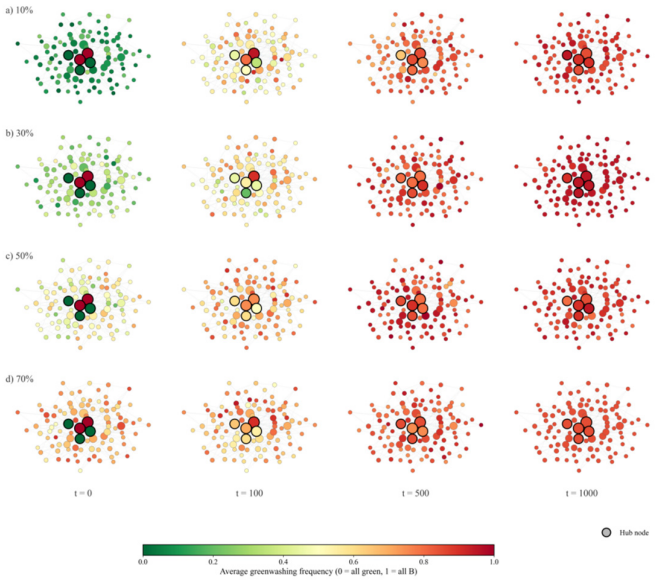



**Figure 14.** Network snapshots of average greenwashing frequency under different initial ratios.

Figure 14 presents the spatial evolution of greenwashing strategies under the four initial ratios at $t$ = 0, 100, 500, and 1000. Node colors indicate the average greenwashing frequency across Monte Carlo replicates for the displayed network, while the hub nodes are highlighted with black outlines.

Under the 10% initial ratio, the network starts from a relatively green state and turns greenwashing-dominant after approximately 500 steps. Under the 70% initial ratio, the network starts with an orange-red dominance and turns almost entirely deep red by $t$ = 1000. The differences in spatial distribution among the four scenarios gradually shrink in the mid-to-late stage, and all four exhibit a greenwashing-dominant pattern at $t$ = 1000.

## 6. Conclusions and prospects

### *6.1. Research conclusions*

Taking the new energy vehicle power battery supply chain as an illustrative application context, this study develops an evolutionary game model on a BA scale-free network by integrating triangular fuzzy payoff representations, degree-dependent strategic inertia, and bounded-rationality Fermi imitation. Through theoretical analysis and repeated Monte Carlo simulations, the study examines how the network structure, strategies' initial placement, payoff uncertainty, and behavioral mechanisms jointly influence greenwashing's evolution. The main findings are summarized as follows.

First, the network position and initial placement of the strategy substantially influence greenwashing's evolution, but hub nodes do not unconditionally determine the final state. The results indicate that highly connected enterprises may influence diffusion through local interactions, accumulated payoffs, and greater strategic inertia. When the same number of initially greenwashing enterprises is assigned to high-degree, randomly selected, and low-degree nodes, substantial differences in terminal greenwashing density are observed. These differences indicate that the location of initial strategies matters beyond their overall number, although the effect remains conditional on the network relationships and payoff evaluation mechanisms. Furthermore, Experiment 6 shows that greenwashing-dominant outcomes occur across initial peripheral greenwashing ratios of 10%, 30%, 50%, and 70%. The overall Friedman test identifies a statistically significant difference ($p$ = 0.01648), but none of the pairwise comparisons remains significant after Holm adjustment. These results support a conditional interpretation of robustness to the initial conditions rather than independence from the initial proportions of the strategy.

Second, uncertain payoffs influence evolutionary incentives, but changes in the payoff bounds do not universally determine convergence outcomes. The theoretical analysis indicates that increasing the optimistic bound of speculative greenwashing returns strengthens the relative incentive for greenwashing, whereas increasing the pessimistic bound of genuine green returns weakens that incentive. The extreme boundary experiments produce higher terminal greenwashing densities than the baseline configuration. However, these adjustments also change the corresponding central payoff values, so their effects cannot be attributed solely to uncertainty width. Under the tested mean-controlled configurations, differences in the payoff interval width are not statistically significant. In addition, the stochastic payoff sampling experiments show that the temporal persistence of payoff realizations can affect the evolutionary outcomes. These findings emphasize the importance of distinguishing fuzzy payoff representations, deterministic defuzzification, and probabilistic payoff sampling.

Third, social learning intensity and strategic inertia influence local strategy updating, but their network-level effects are conditional. The inertia-modified Fermi rule shows that increasing learning intensity raises the probability of imitating a neighbor with a higher payoff while reducing the

probability of imitating one with a lower payoff. Greater inertia lowers the switching probability for a given payoff difference. The numerical results identify overall statistically significant differences associated with learning intensity and inertia. However, terminal greenwashing density does not increase monotonically with learning intensity. Moreover, the formal interaction comparison does not identify a statistically significant learning intensity × inertia effect under the tested configurations ($p = 0.1165$). Therefore, the findings do not establish universally optimal learning intensity or inertia levels.

Fourth, the influence of network connectivity depends partly on payoff evaluation and behavioral mechanisms. Increasing the BA attachment parameter is associated with higher terminal greenwashing density under accumulated payoffs, whereas degree-normalized payoff comparisons substantially attenuate differences across network configurations. Additional robustness tests indicate that finite-horizon terminal outcomes are sensitive to the network size, although lower absorption rates in larger networks limit conclusions about their long-run behavior. Hub count and alternative inertia specifications do not produce statistically detectable overall differences within the tested designs. Furthermore, mechanism ablation experiments show that the magnitude of the initial placement effect varies with payoff normalization and inertia assumptions. These findings suggest that the observed influence of network position cannot be attributed exclusively to connectivity or a universally independent hub anchoring mechanism.

Finally, homogeneous analytical equilibria and finite-network stochastic outcomes must be distinguished. Under the baseline weighted-defuzzified payoffs, the homogeneous replicator model has an attracting interior equilibrium at a greenwashing density of $f^* = 0.8889$. However, finite BA network simulations may reach all-green or all-greenwashing absorbing states or remain nonabsorbed within the observation horizon. The analytical equilibrium therefore serves as a benchmark for understanding relative strategic incentives rather than an exact prediction of stochastic network terminal states.

Overall, this study contributes to supply chain greenwashing research by examining the conditional influence of the initial network position, distinguishing fuzzy payoff representations from probabilistic payoff realizations, and identifying how payoff accumulation and behavioral assumptions shape the relationship between network connectivity and greenwashing's evolution. The resulting framework provides a basis for analyzing heterogeneous strategic interactions and evaluating network-sensitive governance approaches without assuming deterministic convergence or universally optimal intervention strategies.

### *6.2. Managerial implications and policy recommendations*

The findings offer several implications for supply chain managers and regulatory authorities seeking to mitigate greenwashing.

First, prioritize the identification and monitoring of structurally influential enterprises without relying exclusively on hub-based regulation. Enterprises occupying highly connected positions may have greater opportunities to affect neighboring firms' strategic behavior. Regulatory authorities may therefore consider network connectivity and supply chain relationships as supplementary criteria when allocating monitoring resources. However, the results also indicate that high connectivity alone does not guarantee network-wide green adoption. Monitoring priorities should additionally consider actual transaction relationships, observed environmental behavior, and the potential for misconduct to spread through particular supply chain connections. For example, network centrality indicators could be

combined with transaction volume and environmental disclosure history to inform risk-based monitoring priorities.

Second, improve the relative economic incentives for genuine green practices while reducing opportunities for speculative greenwashing. The payoff analysis suggests that limiting the potential returns from misleading environmental claims and strengthening credible incentives for genuine green production may shift relative strategic incentives toward more responsible behavior. Relevant measures may include independent environmental verification, transparent green financing criteria, consistent enforcement, and more predictable support for verified green investments. Nevertheless, the effectiveness of these measures should be evaluated under different payoff and network conditions rather than assumed to ensure universal green convergence.

Third, strengthen the credibility of environmental information transmitted through supply chain relationships. The Fermi imitation mechanism indicates that enterprises may respond more strongly to perceived payoff advantages when social learning intensity increases. Consequently, more intensive information exchange does not necessarily promote genuine green practices if misleading environmental claims remain credible or economically attractive. Supply chain managers and regulators should therefore improve the reliability of environmental disclosures, develop traceable verification procedures, and reduce the information asymmetry associated with unsubstantiated green claims.

Fourth, account for differences in enterprises' strategic adjustment capacities. The baseline degree-dependent inertia mechanism suggests that highly connected enterprises may exhibit greater resistance to short-term changes in incentives under the assumptions of the model. However, alternative inertia specifications do not establish that this degree-dependent relationship holds universally. Governance strategies should therefore consider actual organizational adjustment costs, strategic persistence, and firms' capacity to respond to regulatory changes rather than infer inertia exclusively from the network degree. Combining credible long-term incentives with consistent monitoring may be more appropriate than relying solely on short-term interventions.

Taken together, these recommendations support a differentiated approach to greenwashing governance that considers network position, payoff incentives, information credibility, and behavioral heterogeneity. They should be interpreted as policy implications derived from a stylized evolutionary model rather than empirically established optimal regulatory interventions.

### *6.3. Research limitations and future outlook*

Although the proposed framework provides insights into greenwashing's evolution under network heterogeneity and payoff uncertainty, several limitations should be acknowledged.

First, the network structure is stylized and static. The study uses BA networks to represent heterogeneous enterprise connectivity rather than reconstructing observed transaction relationships among power battery supply chain firms. Real-world supply chains may exhibit changing partnerships, contractual asymmetry, and directed or weighted transactions that are not explicitly represented in the current model. Future research could use empirical supply chain networks and adaptive network models to examine the co-evolution of enterprise strategies and business relationships.

Second, the payoff parameters and behavioral assumptions are illustrative. The triangular fuzzy payoff specifications and degree-dependent strategic inertia are designed to investigate theoretical mechanisms rather than being directly calibrated from firm-level financial or behavioral data. In particular, the assumed positive relationship between network connectivity and strategic inertia

requires empirical validation. In addition, the triangular probability distributions used for stochastic payoff sampling constitute separate modeling assumptions rather than distributions derived from fuzzy membership functions or observed payoff data. Future studies could combine environmental disclosure records, supply chains' transaction data, and firm-level evidence on strategic adjustments to calibrate payoff distributions and behavioral parameters more precisely.

Third, the numerical findings are conditional on the tested network configurations, parameter ranges, and simulation horizons. Although the sensitivity experiments investigate different BA attachment parameters, network sizes, initial strategy placements, payoff evaluation mechanisms, and inertia specifications, the analysis remains based on finite networks and a limited range of alternative models. In particular, simulations that have not reached homogeneous absorbing states within 1000 time steps cannot be interpreted as having converged to stable mixed equilibria. Differences in absorption rates across network sizes also limit direct comparisons of long-run convergence. Future research could examine longer observation horizons, larger networks, alternative topological structures, and additional statistical comparisons.

Fourth, the framework does not explicitly model external governance actors or adaptive learning. Regulatory pressure is represented indirectly through payoff specifications, while government agencies, certification institutions, and consumers are not included as independent strategic agents. Moreover, the model uses local Fermi imitation rather than reinforcement learning or experience-weighted updating. This modeling choice reflects the assumption that enterprises adjust their strategies through local payoff comparisons rather than learning directly from accumulated individual experience. Future research could extend the framework to multilayer governance networks and compare social imitation with experience-based or reinforcement learning mechanisms.

These extensions would help assess the empirical applicability and generalizability of the framework while supporting more comprehensive evaluations of governance strategies for supply chain greenwashing.

## Data and code availability

The Python source code for the six numerical experiments is publicly available in the GitHub repository: https://github.com/huxianrong001/Supply_Chain_Greenwashing_Reproducibility. The repository provides the simulation's implementations for examining the initial placement of the strategy, fuzzy payoff uncertainty, payoff boundary sensitivity, social learning intensity, network heterogeneity, and initial greenwashing proportions.

## Author contributions

Xianrong Hu: Conceptualization, methodology, investigation, data curation, software, validation, visualization, writing–original draft; Haiping Ren: Conceptualization, methodology, formal analysis, writing–review and editing; Fan Zhang: Investigation, writing–review and editing. All authors have read and approved the final version of the manuscript.

## Use of generative AI tools declaration

The authors declare that DeepSeek was used only to polish sentences, correct grammatical errors, and improve linguistic clarity in this manuscript. All research content is original, and the authors take full responsibility for the final published article.

## Acknowledgments

The authors acknowledge that this research received no specific external funding.

## Conflict of interest

All authors declare no conflicts of interest in this paper.

## References

1. Y. Gao, M. Zhang, M. A. Nasir, Y. Yan, J. Wu, L. Zhang, ESG greenwashing behaviour in the electric vehicle supply chain: Insights from evolutionary game theory, *Int. J. Prod. Econ.,* **289** (2025), 109798. https://doi.org/10.1016/j.ijpe.2025.109798
2. C. Liu, X. Gao, S. Dong, Supply chain green gap and firm greenwashing: An institutional isomorphism perspective within the supply chain field, *Supply Chain Manag.,* **30** (2025), 799–817. https://doi.org/10.1108/SCM-03-2025-0226
3. Y. Wei, J. Tang, H. He, C. Wu, M. Lin, H. Xie, Customer concentration and corporate greenwashing, *Res. Int. Bus. Financ.,* **79** (2025), 103090. https://doi.org/10.1016/j.ribaf.2025.103090
4. R. Su, J. Du, S. Jin, Green transformation or speculative greenwashing: Strategy choice of high-carbon enterprises from the perspective of financial support, *Enterp. Econ.,* **42** (2023), 139–149. https://doi.org/10.13529/j.cnki.enterprise.economy.2023.12.014
5. M. Zhou, Z. Y. Zhou, Q. Liu, Green funds and corporate greenwashing: Purifying or fueling the fire, *Finance Account. Mon.,* **45** (2024), 75–83. https://doi.org/10.19641/j.cnki.42-1290/f.2024.14.012
6. X. Y. Lu, H. Y. Pan, F. Xin, Motivation and governance mechanisms of corporate greenwashing based on peer imitation in ESG disclosure, *China Popul. Resour. Environ.,* **35** (2025), 116–128. https://doi.org/10.12062/cpre.20241116
7. Y. Chen, D. Liu, H. He, L. Li, Peer effects of ESG greenwashing within board networks, *Int. Rev. Financ. Anal.,* **106** (2025), 104540. https://doi.org/10.1016/j.irfa.2025.104540
8. N. Guo, D. H. Chen, J. Zhang, Can the digital coupling of banking and enterprises curb corporate ESG greenwashing, *Guizhou Soc. Sci.,* **12** (2024), 122–132. https://doi.org/10.13713/j.cnki.cssci.2024.12.010
9. W. N. Zhao, Y. Chen, T. K. Zhang, The emission permit system and corporate ESG greenwashing, *Macroeconomics,* **4** (2025), 112–127. https://doi.org/10.16304/j.cnki.11-3952/f.2025.04.005
10. H. Zhang, M. D. Jiang, Z. T. Wu, How does digital environmental monitoring affect corporate greenwashing: An analysis based on dual internal and external governance mechanisms, *Ind. Econ. Res.,* **2** (2026), 129–142. https://doi.org/10.13269/j.cnki.ier.2026.02.004
11. J. Xue, R. Li, Y. Li, L. Zhao, A dynamic evolutionary game to discourage enterprise greenwashing, *J. Clean. Prod.,* **477** (2024), 143823. https://doi.org/10.1016/j.jclepro.2024.143823
12. X. Hao, T. Tian, L. Dong, C. W. Y. Wong, K. Lai, Unmasking greenwashing in ESG disclosure: Insights from evolutionary game analysis, *Ann. Oper. Res.,* **356** (2026), 667–695. https://doi.org/10.1007/s10479-025-06538-3
13. P. Majumdar, B. C. Giri, Investment decisions in blockchain and big data information services for mitigating greenwashing in closed-loop supply chains: A tripartite evolutionary game model, *Appl. Soft Comput.,* **188** (2026), 114439. https://doi.org/10.1016/j.asoc.2025.114439

14. A. L. Barabási, R. Albert, Emergence of scaling in random networks, *Science,* **286** (1999), 509–512. https://doi.org/10.1126/science.286.5439.509
15. F. C. Santos, J. M. Pacheco, Scale-free networks provide a unifying framework for the emergence of cooperation, *Phys. Rev. Lett.,* **95** (2005), 098104. https://doi.org/10.1103/PhysRevLett.95.098104
16. M. A. Nowak, R. M. May, Evolutionary games and spatial chaos, *Nature,* **359** (1992), 826–829. https://doi.org/10.1038/359826a0
17. G. Szabo, G. Fath, Evolutionary games on graphs, *Phys. Rep.,* **446** (2007), 97–216. https://doi.org/10.1016/j.physrep.2007.04.004
18. Z. Zhou, T. Li, The co-evolution of information sharing behavior and motivation: A resilience perspective on complex supply chain networks, *Chaos Solit. Fractals,* **208** (2026), 118246. https://doi.org/10.1016/j.chaos.2026.118246
19. X. Wu, E. Shu, D. Ye, S. Zhou, H. Sun, Study on green packaging diffusion in logistics enterprise clusters based on complex network evolutionary game, *J. Clean. Prod.,* **499** (2025), 145166. https://doi.org/10.1016/j.jclepro.2025.145166
20. X. Chen, W. Yang, R. Zhang, Green innovation diffusion based on complex network evolutionary game, *Manag. Decis. Econ.,* **45** (2024), 1215–1229. https://doi.org/10.1002/mde.4060
21. T. Yang, C. Ma, X. Mi, Blockchain-enabled green supply chain development from a complex network evolutionary perspective, *Comput. Ind. Eng.,* **197** (2024), 110548. https://doi.org/10.1016/j.cie.2024.110548
22. D. Dubois, H. Prade, Possibility theory, probability theory and multiple-valued logics: A clarification, *Ann. Math. Artif. Intell.,* **32** (2001), 35–66. https://doi.org/10.1023/A:1016740830286
23. N. Khalil, I. Leyva, J. A. Almendral, I. Sendiña-Nadal, Deterministic and stochastic cooperation transitions in evolutionary games on networks, *Phys. Rev. E,* **107** (2023), 054302. https://doi.org/10.1103/PhysRevE.107.054302
24. L. Cheng, M. Zhang, K. Wang, M. Yuan, Z. Liu, J. Wang, et al., Evolutionary smart contracts for virtual power plant trading: Integrating prospect theory and multi-stage negotiation in cross-regional energy markets, *Int. J. Electr. Power Energy Syst.,* **173** (2025), 111453. https://doi.org/10.1016/j.ijepes.2025.111453
25. L. Cheng, M. Li, C. Tan, P. Huang, M. Zhang, R. Sun, Computational game-theoretic models for adaptive urban energy systems: A review, *Arch. Comput. Methods Eng.,* **33** (2026), 2037–2114. https://doi.org/10.1007/s11831-025-10364-y
26. K. Wang, L. Cheng, M. Yin, K. Zhang, R. Wang, M. Zhang, et al., Evolutionary game theory in energy storage systems: A systematic review, *Sustainability,* **17** (2025), 7400. https://doi.org/10.3390/su17167400
27. C. Liu, W. Li, L. Chang, Q. Ji, How to govern greenwashing behaviors in green finance products: A tripartite game approach, *Financ. Innov.,* **10** (2024). https://doi.org/10.1186/s40854-023-00549-4
28. L. Wang, Z. Y. Li, Y. F. Sha, Synergy governance or collusion fraud: Heterogeneous institutional co-ownership and corporate greenwashing, *Collect. Essays Finance Econ.,* **8** (2023), 70–80. https://doi.org/10.13762/j.cnki.cjlc.2023.08.005
29. J. X. Wang, Z. M. Cao, Can digital transformation restrain greenwashing behavior of enterprises, *J. Hunan Univ. Soc. Sci.,* **38** (2024), 58–67. https://doi.org/10.16339/j.cnki.hdxbskb.2024.02.008
30. S. Y. Yan, J. H. Tan, S. X. Zhang, Green credit interest subsidy policy and the governance of greenwashing in heavy-polluting enterprises, *Finance Econ.,* **12** (2025), 31–45. https://doi.org/10.27041/j.cnki.cjkx.2025.12.004

31. J. Zeng, T. Huang, X. Wu, T. Liu, Authentic or spurious: Evolutionary game of manufacturing greenwashing under dynamic government regulation, *Humanit. Soc. Sci. Commun.,* **12** (2025), 1307. https://doi.org/10.1057/s41599-025-05630-0
32. H. L. Han, The impact of independent directors' environmental background on corporate greenwashing behavior, *Chin. Certif. Public Account.,* **5** (2026), 49–58. https://doi.org/10.16292/j.cnki.issn1009-6345.2026.05.017
33. J. Y. Cui, S. Q. Xu, X. Na, L. M. Pan, L. Y. Lü, Supply chain research based on complex network theory, *Acta Phys. Sin.,* **73** (2024), 198901. https://doi.org/10.7498/aps.73.20240702
34. F. Ding, H. Chen, Supply chain network modeling research from the perspective of complex networks, *J. North Univ. China Nat. Sci. Ed.,* **39** (2018), 120–127. https://doi.org/10.3969/j.issn.1673-3193.2018.02.003
35. Z. Zhao, G. Zhou, R. Pan, Study on local world evolution model of weighted complex supply chain network based on location attraction, *Comput. Sci.,* **45** (2018), 71–76.
36. W. B. Cao, X. Xiong, Local-world evolution model of complex supply chain networks under edge benefits, *Appl. Res. Comput.,* **1** (2016), 75–77. https://doi.org/10.3969/j.issn.1001-3695.2016.01.017
37. R. Zhang, L. Li, Research on evolutionary game and simulation of information sharing in prefabricated building supply chains, *Sustainability,* **15** (2023), 9885. https://doi.org/10.3390/su15139885
38. X. J. Wang, Overview of evolutionary games and their learning mechanisms and evolutionary dynamics on complex networks, *Yuejiang Acad. J.,* **13** (2021), 70–84. https://doi.org/10.13878/j.cnki.yjxk.20210521.003
39. G. Wu, X. Chen, X. Niu, Complex network evolutionary games of green technology innovation incorporating prospect theory, *Manag. Decis. Econ.,* **46** (2025), 1774–1791. https://doi.org/10.1002/mde.4468
40. Y. Duan, J. Huang, J. Zhang, Public goods games with long-term payoff mechanisms in heterogeneous networks, *Chaos Solit. Fractals,* **174** (2023), 113862. https://doi.org/10.1016/j.chaos.2023.113862





AIMS Press

© 2026 the Author(s), licensee AIMS Press. This is an open access article distributed under the terms of the Creative Commons Attribution License (https://creativecommons.org/licenses/by/4.0)